Review article

Control approaches of power electronic converter interfacing grid-tied PMSG-VSWT system: A comprehensive review

Hussein Shutari [a,*], Taib Ibrahim [a], Nursyarizal Bin Mohd Nor [a], Yahya Z. Alharthi [b], Hakim Abdulrab [c,*]

[a] *Department of Electrical and Electronic Engineering, Universiti Teknologi PETRONAS, Seri Iskandar, 32610, Perak, Malaysia*
[b] *Department of Electrical Engineering College of Engineering, University of Hafr Albatin, Hafr Al Batin, 39524, Saudi Arabia*
[c] *School of Electrical Engineering and Artificial Intelligence, Xiamen University Malaysia, Selangor, 43900, Malaysia*

ARTICLE INFO

ABSTRACT

The growing interest in wind power technology is motivating researchers and decision-makers to focus on maximizing wind energy extraction and enhancing the quality of power integrated into the grid. Over the past decades, significant advancements have been made in Wind Energy Conversion Systems (WECS), such as moving to variable speed wind turbines (VSWT), using various generator types, and interfacing with many power electronic converter topologies. Recently, the majority of wind turbine industries have adopted the VSWT, which is based on the permanent magnet synchronous generator (PMSG) and incorporates a fully controlled power electronic converter (FCPEC) topology due to its notable features of full controllability, ultimately enhancing the efficiency and power quality of the WECS. This paper presents a concise overview of the PMSG-VSWT system and comprehensively reviews the most recent control approaches developed for the FCPEC that play a crucial role in the operation and performance of the PMSG-VSWT system. The paper begins with a comprehensive review of the Maximum Power Extraction Algorithms (MPEA) used in the PMSG-VSWT system, as reported in esteemed research articles over recent years. It investigates the fundamental concepts of each MPEA, examining their advantages and disadvantages, providing critical comparisons, highlighting related work, and discussing the advancements achieved in this field. Subsequently, the paper reviews the prevalent control schemes for the Grid-Side Inverter and Machine-Side Rectifier (GSI/MSR) in the FCPEC. It covers common control approaches such as vector control, direct control, sliding mode control, and model productive control, including modern and intelligent techniques. Additionally, the paper details recent improvements and approaches adopted to address challenges in these common schemes, involving optimizing algorithms and adaptive techniques. The paper provides essential insights into trends, improvements, and challenges in the domain and acts as a crucial reference for researchers working with PMSG-VSWT systems.

---

* Corresponding authors.
  E-mail addresses: Shutari2000@outlook.com (H. Shutari), Hakim.abdulrab@xmu.edu.my (H. Abdulrab).

1. Introduction

Indeed, the rapid expansion of population, technological advancement, and industrialization has led to an increase in energy demand during recent years [1]. This demand causes a significant increase in electricity production, which is mostly dependent on fossil fuel supplies [2]. More use of fossil fuels has a negative effect on global warming, climate change, and the trade deficit [3,4]. This situation pushed the utilities and policymakers to look at renewable energy sectors for providing sustainable and green electricity [5–9]. Wind power generation has been identified as the fastest growing renewable energy technology, with the development of a large capacity of wind turbines, electric generators, and sophisticated power electronics interfaces [10]. It is also regarded as one of the most lucrative means of generating electricity from renewable sources. Thus, the installed capacity of wind energy conversion systems (WECS) has expanded from a few MW to hundreds of GW during the last couple of decades as displayed in Fig. 1 [11]. Moreover, the Global Wind Energy Council indicates that By 2030, 29.1% of the world's energy is expected to come from WECS [12].

In WECS, the Wind Turbine (WT) stands as a crucial component, classified into Variable Speed Wind Turbine (VSWT) and Fixed Speed Wind Turbine (FSWT) based on the handled wind speeds. VSWTs have gained significant interest in the modern wind energy sector due to their distinctive features, such as maximum power extraction, reduced ripple, and controllability compared to FSWT [13]. Within the wind power sector, various generators come with VSWTs, including Permanent Magnet Synchronous Generators (PMSGs) [14], Squirrel Cage Induction Generators (SCIGs) [15], and Doubly-fed Induction Generators (DFIGs) [16]. The VSWT relies on PMSG, and a Full-Scale power Electronic Converters (FSPEC) topology has been widely adopted by most wind turbine industries [17]. Different FSPEC topologies are utilized in this system, such as diode rectifiers, Fully Controlled Power Electronic Converters (FCPEC), Vienna rectifiers, Z-Source Inverters, multilevel converters, and matrix converters [18]. Each topology has distinct advantages and disadvantages, contributing uniquely to the system's performance and enhancing efficiency and stability in wind energy conversion [19]. However, the FCPEC, featuring two voltage source converters connected back-to-back via a DC-link capacitor, is considered highly effective. It ensures complete controllability, decoupling the PMSG from grid disruptions for stable performance. The topology of FCPEC comprises a Machine-Side Rectifier (MSR) and a Grid-side Inverter (GSI), with three main control schemes: MSR controller, Maximum Power Extraction (MPE) algorithm, and GSI controller [20]. Each of the control schemes has its own technology and respective control objectives. The effectiveness of these schemes is a crucial point for achieving optimal conversion efficiency from the wind, adhering to utility grid interconnection standards, and quality of wind power integration [21–24].

In the domain of control schemes introduced for FCPEC, an extensive body of research has been conducted to enhance both MPEAs and MSR/GSI control schemes. This comprehensive body of work is well-documented across numerous review papers. Despite these significant advancements, a critical gap persists in the existing body of literature, where most current articles review either focus solely on MPE algorithms [25–28] or MSR/GSI control schemes [29–31]. While some attempt to explore both aspects, their reviews often remain cursory, lacking in-depth insights [29]. Additionally, they tend to limit their scope to related areas and frequently overlook the essential approaches that are used as the basis of these control schemes [32,33]. Therefore, considering the ongoing research and advancements in the field, a review paper that investigates and analyzes the existing body of work on both MPE algorithms and MSR/GSI control schemes in FCPEC systems and the advancements that have been achieved up to date is valuable. Motivated by this concern this paper will explore comprehensive exploration and synthesis of the recent MPE algorithms along with the most recent MSR/GSI control schemes and their associated approaches used for FCPEC. Emphasizing improvements over previously published works, this paper outperforms prior literature reviews through a more comprehensive and modern exploration. While existing works may briefly introduce MPE algorithms and control schemes, the contribution here presents a comprehensive and up-to-date knowledge of each MPE algorithm. This includes elucidating their working principles, advantages, and disadvantages, with the inclusion of schematic diagrams for enhanced clarity, as well as an outline of the most recent related research and improvements
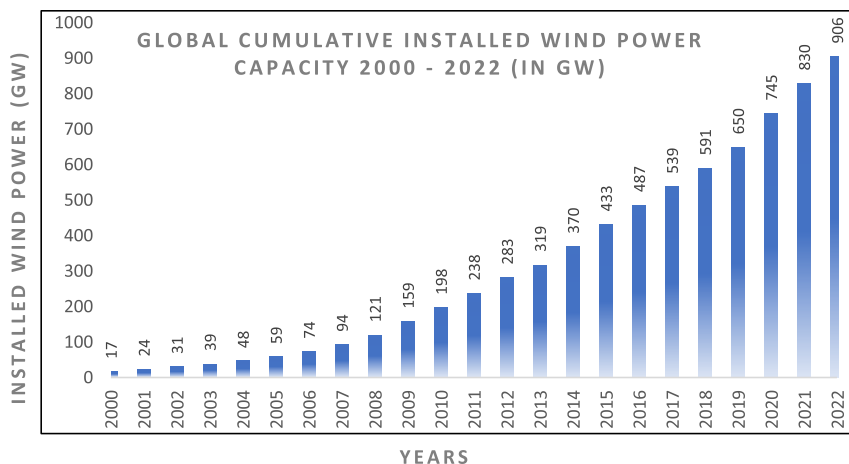

Fig. 1. Globally installed wind power capacity.

Table 1
List of abbreviations.

Abbreviation	Description	Abbreviation	Description
ANN	Artificial Neural Network	ORB	Optimal Relationship Based
AP	Active Power	OTC	Optimum Torque Control
AP&O	Amended Perturb and Observe	P&O	Perturb and Observe
CCS	Continuous Control Set	PCC	Point of Common Coupling
DB-MPC	Deadbeat Model Predictive Control	PIC	Proportional-Integral Control
DFIG	Doubly Fed Induction Generators	PMSG	Permanent Magnet Synchronous Generator
DPC	Direct Power Control	PSF	Power Signal Feedback
FCPEC	Full Controlled Power Electronic Converter	RAP	Reactive Power
FLC	Fuzzy Logic Control	SCIG	Squirrel Cage Induction Generators
FOC	Field Oriented Control	SMC	Slide Mode Control
GSI	Grid Side Inverter	SO-SMC	Second Order Slide Mode Control
HSS	Hybrid Step Size	SP&O	Standard Perturb and Observe
HO-SMC	Higher-order Slide Mode Control	ST-SMC	Super-Twisting Slide Mode Control
IMSAF	Improved Mean Square Auto-Frequency	SVM	Space Vector Modulation
INC	Incremental Conductance	TSR	Tip Speed Ratio
ISMC	Integral Slide Mode Control	UG	Utility Grid
LuT	Lookup Table	VSS	Variable Step Size
MPEA	Maximum Power Extraction Algorithm	VOC	Voltage Oriented Control
MSR	Machine Side Rectifier	VSWT	Variable Speed Wind Turbine
PPT	Parabolic Prediction Technique	WECS	Wind Energy Conversion System

Table 2
List of nomenclature.

Abbreviation	Description	Abbreviation	Description
Cp	Power Coefficient	V_ω	Wind speed
Pn	Number of Poles	A	Swept Area
J	Moment of Inertia	P_{wind}	Available Wind Power
T_e	Electromagnetic Torque	P_{con}	Converted Wind Power
D	Damping Coefficient	ρ	Air Density
ω_e	Electrical Angular Speed	V_{w-in}	Cut-in Wind speed
R	Blade Radius	V_{w-out}	Cut-out wind speed
ω_m	Mechanical Rotational Speed	T_{opt}	Optimal Torque
λ_{opt}	Optimal Tip Speed Ratio	P_{dc}	DC link Power
β	Pitch Angle	V_{dc}	DC-Link Voltage

that have been achieved. Furthermore, this study goes a detailed exploration of control approaches that serve as the basis for the MSR/GSI control schemes. This investigation encompasses optimization algorithms, smart techniques, sliding mode control, model predictive control, and other modern methods, providing insights into their working principles, advantages, disadvantages, and the latest related research. This serves as an essential resource, offering valuable insights and guiding future research by consolidating comprehensive information in one source.

The remaining sections of the paper are outlined as follows: Section 2 details the review methodology of this paper. Section 3 overviews the WECS technology. Section 4 presents the configuration, modeling, and control schemes of FCPEC interfacing with the PMSG-VSWT. Section 5 provides exhaustive reviews of the MPEA used with FCPEC. Section 6 extensively covers the control schemes and associated approaches developed for both MSR and GSI. Section 7 discusses potential research directions. Finally, the article is concluded in section 8. The abbreviations and nomenclatures used throughout this paper are listed in Table 1 and Table 2 respectively.

2. Review methodology

To comprehensively review the control approaches employed in power electronic converters for PMSG-VSWT systems, a rigorous and balanced review methodology was implemented. This methodology passed through three stages of screening:

Initial Screening: In the first stage, the authors focused on identifying review articles related to control schemes for PMSG-based VSWT systems. The main keywords used included "WECS, "Control," and "PMSG". The search strings constructed from these keywords were applied using databases including, Google Scholar, IEEE Xplore, ScienceDirect, Scopus, and Web of Science. The query used was: ("Wind Energy Conversion System" OR "Variable Speed Wind Turbine") AND "PMSG" AND ("Control Strategy" OR "Control Approach" OR "Control Method" OR "Control Scheme" OR "Control Technique"). Boolean operators like AND and OR were utilized to combine different terms effectively, aiming to identify relevant literature for the review. The selected literature was limited to publications from the past 15 years (2008-2023) to focus on review papers that highlight the main control schemes and identify research gaps. After a relevance analysis based on keywords and publication dates, only indexed and highly cited articles were selected for thorough review. This stage provided deep insights into control schemes for power electronic converters, revealing three main control systems: MPEA, MSR, and GSI control schemes. Moreover, it identified that the MSR and GSI are mainly

controlled by schemes based on either Sliding Mode Control (SMC), Model Predictive Control (MPC), field-oriented control (FOC), voltage-oriented control (VOC), direct torque control (DTC), or direct power control (DPC). These findings paved the way for the subsequent stages of the screening.

MPEA-Focused Screening: The second stage focused on identifying papers related to MPE algorithms for PMSG-based VSWT systems to synthesize the advancements and trends of these methods. The search query was: ("Wind Energy Conversion System" OR "Variable Speed Wind Turbine") AND "PMSG" AND "MPEA OR MPPT". The search encompassed reputable scientific databases, including Google Scholar, IEEE Xplore, ScienceDirect, Scopus, and Web of Science. This stage prioritized papers published from 2015 to 2023 to ensure the inclusion of recent advancements and emerging trends. Papers with high citation counts and those published in reputable journals were given higher significance. The selected literature was analyzed based on several parameters, including the type of MPE algorithm used and the common evaluation metrics. The analysis involved categorizing papers to identify common approaches and innovative techniques.

MSR/GSI Control Schemes Screening: In the final stage, the authors aimed to refine the search and deeply analyze the control approaches used for MSR and GSI control schemes identified in the first stage. The query used was: ("Wind Energy Conversion System" OR "Variable Speed Wind Turbine") AND "PMSG" AND ("Sliding mode control" OR "Model predictive control" OR "Field-oriented control" OR "Voltage-oriented control" OR "Direct torque control" OR "Direct power control"). The search was conducted through databases also including Google Scholar, IEEE Xplore, ScienceDirect, Scopus, and Web of Science. The selection criteria focused on publications from 2015 to 2023, emphasizing citation frequency and significant contributions to the field. Different approach-based control schemes were comprehensively reviewed and mainly focused on recent improvements and approaches adopted to address challenges in these common schemes, involving optimizing algorithms and adaptive techniques. Key scientific insights were extracted from the selected articles and compared and analyzed based on their objectives, advantages, and limitations in enhancing WECS system performance and efficiency.

3. Wind energy conversion system

The WT is deemed the main element of WECS which in turn converts the kinetic wind energy into mechanical energy and further is transformed into electricity using the associated generator. The WT could be built either for variable or fixed speed operation modes [34,35]. The VSWT recently has gained interest in the modern wind power industry thanks to its own advantages such as harnessing more power and control capability [36,37].

In the wind power sector, several types of electrical machines are employed, each with distinct characteristics and operational efficiencies. Commonly used generators include SCIGs, DFIGs, and PMSGs. SCIGs are known for their simplicity and robustness, although they often lag in efficiency. DFIGs offer improved control and efficiency but come with increased complexity and higher costs. However, PMSGs stand out for their superiority in wind energy applications, offering high efficiency [38]. This advantage is attributed to their design features, such as a gearless construction and a self-excitation system, which reduce maintenance costs. Their capability to generate power at lower wind speeds makes them particularly beneficial. Furthermore, PMSGs offer a broad operational range and high reliability, essential for optimizing wind power generation [39]. Additionally, their full decoupling from the utility grid and capability for comprehensive system controllability play a key role in maximizing wind power production. These generators exhibit a wide operating range, high performance, remarkable reliability, and enhanced fault ride-through capability. The wind turbine industry increasingly prefers the adoption of PMSGs, signifying an essential point in wind energy generation technology [33]. Table 3 compares the different generator-based wind turbines, studying their power output across various wind speeds [18].

Table 3
Comparison of different wind turbine generators across different wind speeds.

Turbine Generators vs wind speed		3	4	6	10	12	13
SCIG	Power (kW)	0.31	0.91	3.59	16.3	27.4	32.3
	Eff. (%)	67	82.8	95.6	93.4	86	86
PMSG	Power (kW)	0.44	1.04	3.56	16.5	27.6	33.2
	Eff. (%)	94.7	94.7	94.7	94.8	94	94
DFIG	Power (kW)	0.39	0.85	2.98	14.2	24.5	29.7
	Eff. (%)	70.5	81.2	89.6	92.3	88	87.5

4. PMSG-VSWT system configuration

The typical configuration of the grid-connected- PMSG-VSWT system includes a VSWT, a PMSG, an FSPEC, and a filter connected to the UG [40]. The FSPEC, comprising an MSR and a GSI is a crucial component for maximizing wind power extraction and ensuring high-quality electricity delivery to the grid. Various FSPEC topologies are employed in this system, such as diode rectifiers, fully controlled back-to-back converters, Z-source inverters, multilevel converters, matrix converters, and Vienna rectifiers [18]. Each topology has its distinct advantages and disadvantages, contributing uniquely to the system's performance and enhancing efficiency and effectiveness in wind energy conversion. For instance, Vienna rectifiers offer the advantages of high power efficiency and low harmonic distortion, making them ideal for maintaining power quality. However, they also have disadvantages like increased
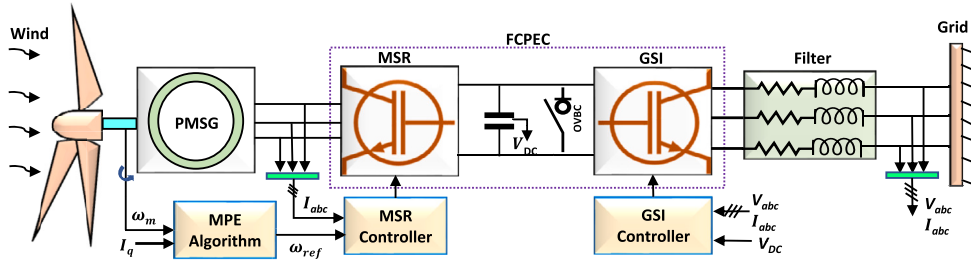
Fig. 2. WECS configuration.

complexity and higher costs. These challenges are being addressed through advanced management techniques, including the use of observers and nonlinear control methods. This in turn helps to optimize performance and mitigate issues associated with their complex nature and sensitivity to parameter variations [41,19,42,43].

This part of the work mainly focuses on the control schemes of the fully controlled power electronic converter as the most commonly investigated in the academic research and wind power sectors. This converter is formed of MSR and a GSI tied together by a DC-link capacitor and associated with three primary control schemes (MPEA, MSR, and GSI control schemes) as revealed in Fig. 2. In this configuration, the wind moves over the WT blade and creates a torque that spins the blades and the linked shaft which in turn drives the turbine generator to produce electricity. This power is provided to the UG via FCPEC obliging the control schemes and filter to fulfill the UG's standards [44].

4.1. VSWT model

Kinetic wind energy is considered the main propulsion source of a VSWT and is given by Equation (1):

$$P_{wind} = 0.5\rho A V_\omega^3 \tag{1}$$

where A describes the swept zone covered by the WT blades (m^2), V_ω denotes the wind speed (m/s), and ρ reflects the density of the air (kg/m^3). Unfortunately, the WT can only harvest a portion of the available wind energy due to physical limitations as stated by Betz Law [45]. The actual amount of harnessed power by WT is determined by Equation (2) [46].

$$P_{con} = 0.5\rho A V_\omega^3 C_p(\beta, \lambda) \tag{2}$$

Equation (2) discloses that the converted wind power depends on the coefficient (C_p) which is a function of pitch angle β and TSR (λ) as defined in Equations (3)-(5).

$$C_p(\lambda, \beta) = 0.22 * (\frac{116}{\lambda_i} - 0.3\beta - 5)e^{\frac{-12.5}{\lambda_i}} \tag{3}$$

$$\frac{1}{\lambda_i} = (\frac{1}{\lambda + 0.08\beta} - \frac{0.035}{\beta^3 + 1}) \tag{4}$$

The λ is the ratio of the turbine's rotational speed (ω_m) to the blade radius (R) at the ambient wind speed (V_ω) and is expressed in Equation (5).

$$\lambda = \frac{\omega_m R}{V_\omega} \tag{5}$$

To capture the most available wind energy, a WT must be driven at the optimum $C_{p.Opt}$ [47]. This can be achieved by obtaining the optimal WT spinning speed for each ambient wind speed, as illustrated in Fig. 3. Part (a) of the figure shows the relative power coefficient to the TSR, and part (b) shows the relationship between the rotational speed of the WT and the extracted wind power under different wind speeds.

4.2. PMSG model

The PMSG takes the mechanical energy from the turbine's rotating shaft and converts it into electricity. This kind of generator possesses characteristics of efficient electrical power density and the least copper loss as a result of the deficiency of field coils. The PMSG's dynamic voltage equations can be expressed in ($dq - axis$) coordinates as defined in Equations (6) and (7).

$$v_{ds} = R_s i_{ds} + L_d \frac{di_{ds}}{dt} - \omega_e L_q i_{qs} \tag{6}$$

$$v_{qs} = R_s i_{qs} + L_q \frac{di_{qs}}{dt} + \omega_e \psi_f + \omega_e L_d i_{ds} \tag{7}$$

where i_{qs}, v_{qs}, i_{ds}, and v_{ds} represent the PMSG's stator current and current voltage. The inductances of the PMSG's stator are represented by L_q and L_d, while the stator resistance is represented by R_s. ψ_f and ω_e stand for the magnetic field and the speed of
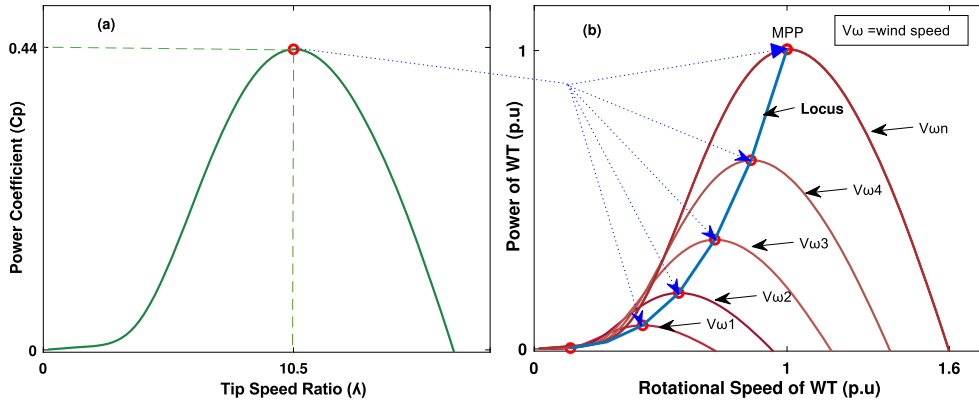
Fig. 3. WT characteristics. (a) Cp vs.TSR (b) Power vs. rotational speed.

the electrical rotation, respectively. The electrical angular speed, denoted by ω_m, is directly related to the PMSG's mechanical speed as a function of the number of poles, P_n, and is defined as follows in Equation (8).

$$\omega_e = P_n \omega_m \tag{8}$$

The Equation (9) can be used to figure out the electromagnetic torque T_e of the PMSG:

$$T_e = \frac{3}{2} P_n [(L_d s - L_q s) i_{ds} i_{qs} - \psi_f i_{qs}] \tag{9}$$

Thus, the dynamic model formula for the PMSG is expressed as Equation (10).

$$J \frac{d\omega_m}{dt} = T_e - T_m - D\omega_m \tag{10}$$

4.3. PMSG-VSWT operating region and control

In WECS, the PMSG-VSWT is restricted to operating only between the cut-in (V_{w-in}) and cut-out (V_{w-out}) wind speed limits. Out of these bounds, the WT should be halted for the safety of the turbine and generator. Considering this, the PMSG-VSWT's operational regions are divided into four distinct operating regions as shown in Fig. 4. Region 1, and Region 4, when the wind speed is below V_{w-in} and above V_{w-out}, respectively, the WT must be parked and disconnected from the UG for safety requirements. Region 2 (the MPE region), when the wind speed is between V_{w-in} speed and rated speed: The MPE control scheme is activated so as to enable wind turbines to capture the maximum available from the wind. Region 3 (pitch angle region), when the wind speed is higher than the rated speed: the pitch angle control is used to reduce mechanical stress on the wind turbine blades and rotational speed is limited at rated values to restrict the mechanical power [48].
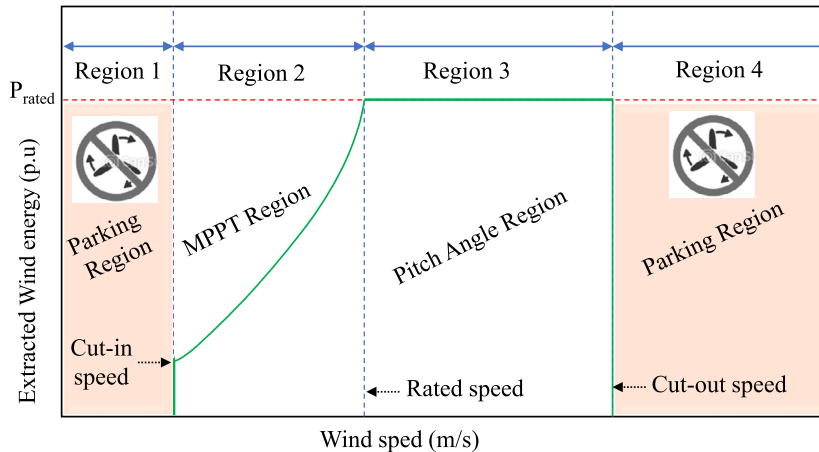

Fig. 4. Operating region of VSWT.

The amount of power generated by PMSG-VSWT mainly depends on upcoming wind speed and the turbine's rotational velocity. To achieve meaningful use of the available wind energy, PMSG-VSWT must be operated at optimum rotational speeds related to

the prevailing wind speed. Meanwhile, the converted wind power is unsuitable for immediate injection into the UG since the grid's voltage has to be constant in both frequency and amplitude. Therefore, integrating PMSG-VSWT systems with power electronic converters and advanced control schemes is crucial for achieving efficient, high-quality, and cost-effective wind power generation and grid integration. [41,49,19].

4.4. Control schemes of FCPEC

In WECS, the amount of power that is converted by WT depends on prevailing wind speed and turbine angular spinning speed ($\omega_{m.opt}$). For any specific WT at every particular wind speed, there is only one $\omega_{m.opt}$ which yields maximum captured wind power [50]. In addition, the generated wind power is inappropriate for direct integration into the UG as the electrical grid's voltage must be stable in both frequency and amplitude [51]. Therefore, an FCPEC with developed control schemes is interfaced as a tie between the PMSG-VSWT system and UG terminals [52]. The FCPEC consist of three main control schemes namely the MPEA, MSR control schemes (MSRCS), and GSI control scheme (GSICS) as outlined in Fig. 2. The MPEA seeks the $\omega_{m.opt}$ for each wind speed and sends the obtained value to the MSRCS. Subsequently, the MSRCS compels the WT to spin at the spinning speed specified by the MPEA. While the GSICS controls the DC-link voltage, terminal voltage and current following the UG framework [53,54]. Sections 5 and 6 extensively review the recent MPEA algorithm and MSRCS/GSICS used for the FCPEC associated with the PMSG-VSWT system.

5. MPE algorithm

The MPE algorithm is an essential element of the WECS control system for getting the best wind energy conversion efficiency. This induced the researchers and scientists to develop and implement many MPE algorithms in the recent literature [55]. The most commonly investigated MPE algorithms are being reviewed in the next subsections.

5.1. TSR-MPE algorithm

The TSR is described as the ratio of the blade tip speed to the speed of the incoming wind speed [56]. For each particular wind turbine, there is a unique optimal TSR that results in maximum power extraction. This optimal TSR (λ_{opt}) is constant and can be kept by obtaining the optimal rotational speed ($\omega_{m.opt}$) for each prevailing wind [57,58]. To achieve this, the TSR-MPE algorithm calculates $\omega_{m.opt}$ using the formula in Equation (11), which depends on the measured wind speed and WT parameters [59–61], as portrayed in Fig. 5.

$$\lambda_{opt} = \frac{\omega_m R}{V_\omega} \tag{11}$$

The wind speed is obtained in two essential ways: either based on physical wind speed sensors or wind speed estimation [62]. For measuring the actual wind speed using physical sensors, many anemometers of 5–10% accuracy are placed around the swept area of WT [63]. As a result, both initial and ongoing costs rise while overall dependability and efficiency fluctuate [64]. To overcome the limitations of anemometers, some scholars use the wind speed estimation (WSE) algorithms [65–68]. These WSE algorithms offer a precise calculation of the actual wind speed; nevertheless, the calculated accuracy specifies the tracking efficacy and power extraction. One of the WSE algorithms, which was developed based on polynomial approaches, is considered simple, rapid, and accurate [69]. In addition, different WSE methods are employed based on smart adaptive controllers or the mathematical modeling of WECS [70,63,71–74]
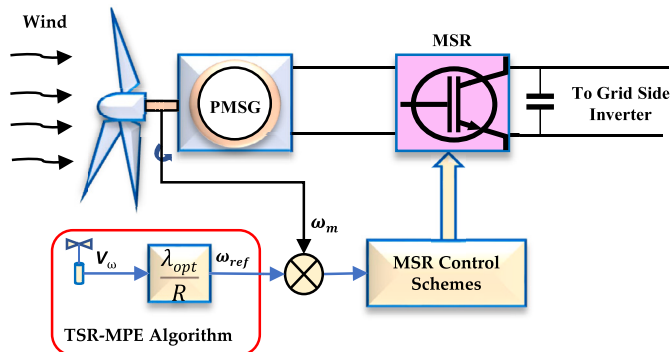

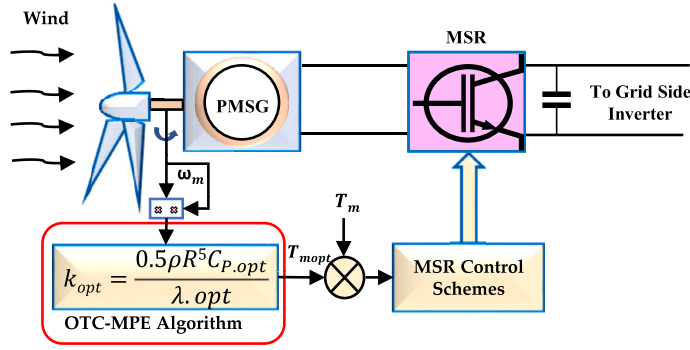**Fig. 5.** The block diagram of the TSR-MPE algorithm.

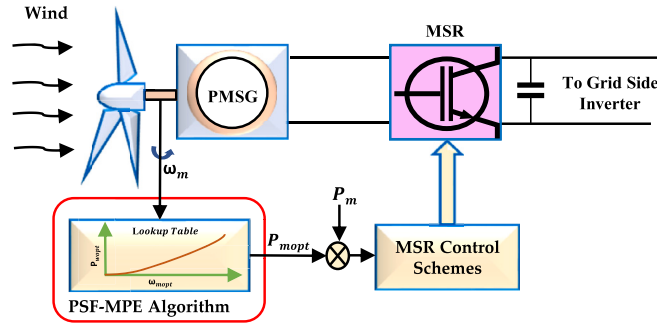**Fig. 6.** The block diagram of the OTC-MPE algorithm.

Fig. 7. The block diagram of the PSF-MPE algorithm.

5.2. OTC-MPE algorithm

The main concept of the OTC-MPE is that the algorithm generates the optimum reference torque of the WT that results in optimum power based on some WT parameter and measuring its rotational speed [75,76]. The ideal relationship between the WT rotational speed (w_m) and the optimal torque (T_{opt}) is given by Equation (12):

$$T_{opt} = k_{opt} * w_m^2 \tag{12}$$

where k_{opt} indicates the WT parameter, which is expressed in Equation (13) as follows:

$$k_{opt} = \frac{1}{2} \rho \pi R^5 \frac{C_{p.opt}}{\lambda_{opt}^3} \tag{13}$$

The block diagram of the OTC-MPE scheme is depicted in Fig. 6. In general, the OTC-MPE is simple, very fast and efficient. However, the efficiency is lower than that of the TSR-MPE because it does not measure the wind speed directly [77,78]. This means that changes in the wind do not immediately and significantly reflect in the reference signal.

Moreover, computing the optimal parameter k_{opt} depends on the turbine characteristic and air density, which may vary considerably with turbine ageing and across various seasons. Inaccurate calculation of k_{opt} makes the tracking trajectory incorrect, and therefore, leads to a considerable loss in output energy [79,80].

5.3. PSF-MPE algorithm

The PSF-MPEA requires previous studies for the optimal output power curve in relation to turbine generator shaft speed [81–83]. This can be achieved via extensive simulations or experimental setups for each WT and the obtained results are recorded in a lookup table (LuT). Then, during the tracking procedure, the optimum reference speed for each precise wind speed is produced from the LuT to attain the maximum power [84,85]. Fig. 7 shows the block diagram of the PSF-MPEA. In some PSF-MPE, the DC-link voltage and maximum DC power are handled as input and output for the LuT to estimate the optimal curve instead of mechanical power vs. shaft speed [86,87]. Consequently, the optimal power curve and actual power are used to accurately estimate $\omega_{m.opt}$ [88,84].

5.4. INC-MPE algorithm

The INC-based MPEA is developed based on the fact that the derivative of DC-link power relative to the DC-link voltage at a maximum point is zero, as described in Equation (14) below [89].
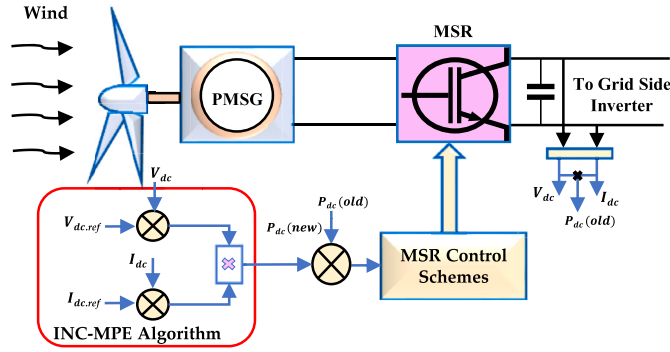
Fig. 8. The block diagram of the INC-MPE algorithm.

$$\frac{dP_{dc}}{dV_{dc}} = 0 \tag{14}$$

Since power is equal to the current multiplied by voltage, the formula for calculating this slope is given by Equation (15).

$$\frac{dP_{dc}}{dV_{dc}} = \frac{d(VI)_{dc}}{dV_{dc}} = 0 \tag{15}$$

By considering the dependence of the DC-link current on the voltage, this condition can be represented in Equation (16).

$$I_{dc} + V_{dc}\frac{dI_{dc}}{dV_{dc}} = 0 \tag{16}$$

Rearranging Equation (16):

$$\frac{I_{dc}}{V_{dc}} = -\frac{dI_{dc}}{dV_{dc}} \tag{17}$$

The essential criterion for the INC-MPEA is defined by Equation (17), stating that the conductance value must equal the incremental conductance value at the MPE condition [90]. Equation (17) also suggests that the maximum power tracking procedure and perturbation direction are achieved solely by monitoring the MSR output power and determining the slope of the power change. Therefore, this technique relies on the DC-link current (I_{dc}) and voltage (V_{dc}) instead of speed sensors and WT characteristics, enhancing system reliability and reducing costs. In the original INC-MPE tracking procedure, the DC-link voltage is adjusted by a fixed step size ΔVdc, and the MSR output power is monitored until an optimal DC-link voltage ($V_{dc.opt}$) maximizing converted power is reached [91]. The schematic diagram of the INC-MPE algorithm is illustrated in Fig. 8. In recent studies, a modified INC-MPE algorithm with a variable step size ΔVdc has been introduced to enhance the performance of the original INC algorithm. This modified algorithm automatically adapts ΔVdc, improving WECS dynamic performance, system accuracy, and convergence speed. However, the step size is constrained, and its alteration depends on the WT generator size and design parameters [91,92]. In other articles, the adaptive INC-MPE algorithm is employed to predict suitable perturbation step sizes, alter perturbation directions, and monitor the maximum power location [93,94].

5.5. ORB-MPE algorithm

The ORB-MPEA working principle is based on establishing optimal relationships between different wind turbine parameters such as turbine rotation speed, output mechanical power, output electrical power, rectified DC voltage, rectified DC current, and so on [45,95–97]. It has the advantage of requiring neither sensor for measuring wind speed, nor a LuT. It acts based on a previously obtained system curve. As a result, it is widely used in WECS's commercial products [98–101]. However, it necessitates a large number of memory places for storing the previously obtained optimum curve relations, which are primarily related to the WECS structure. The high memory requirement is considered a significant disadvantage of the ORB-MPE [102,97,103]. In addition, there are other methods namely the power to optimal speed and power to optimal voltage [18] methods that work based on an online search for maximum power, without considering the associated wind speed. Fig. 9 illustrates the ORB-MPE algorithm's structure.

5.6. SP&O-MPE algorithm

Standard P&O-based MPE is a mathematical optimization technique used to search for the maximum value of a particular function [104,27]. It is widely used in WECS to get the optimal operating point that maximizes the extracted wind energy [96]. The basic concept behind the SP&O-MPEA is that the algorithm perturbs the variable's control in a particular direction by step size Δs and considers the captured power variation. If the captured power value increases, this means the operating point is moving to the optimum point, and then the algorithm continues the perturbation by the same SS and in the same direction. Conversely, if the captured power value after perturbation decreases, this means the operating point is moving away from the optimum point, and
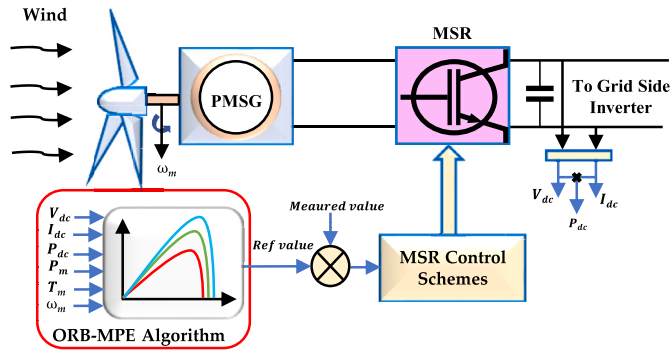
Fig. 9. The block diagram of the ORB-MPE algorithm.
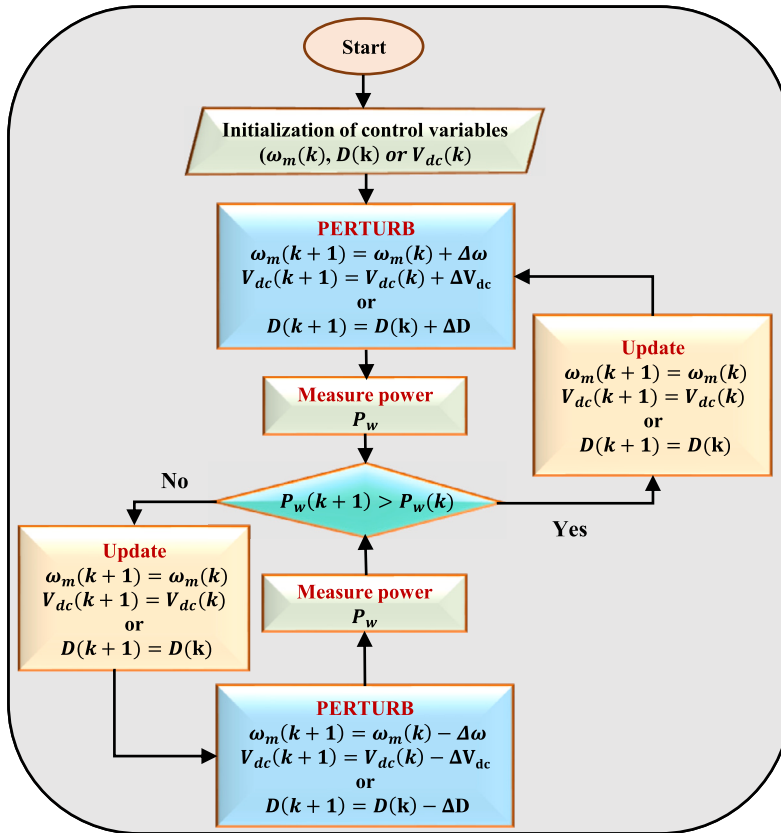
Fig. 10. P&O-MPE algorithm flowchart.

then the algorithm reverses the perturbation direction and by the same step size [105]. In the existing literature, some works were based on perturbing the rotational speed ω_m and observing the mechanical power, (P_w). This methodology, exemplified by the work of Singh et al. in [106], aims to optimize the performance of the investigated system and maximize power extraction from wind energy generation. While others were based on the perturbing the DC-link voltage of the rectifier (ΔV_{dc}) and monitoring the DC-link power (P_{dc}) [107–109] as is exhibited in the flowchart of Fig. 10. In the approach of measuring DC-link output power, the mechanical sensors are not required, and thus they are more reliable and low-cost [67]. Fig. 11 illustrates the block diagram of the P&O-MPEA. The SP&O-PMEA is the most commonly used due to its advantages of being sensor-less, requiring no prior knowledge about the turbine system and being able to find the optimal operating point as wind speeds fluctuate. However, the main drawback of the SP&O-MPE algorithm is the difficulty in selecting the optimal step size (SS). A small SS improves the accuracy of reaching the maximum point (MP) but reduces the convergence speed. Conversely, a big SS results in a faster response but causes oscillations around the optimal operating point, leading to power loss in the WECS, as shown in Fig. 12. Fig. 12 (A) illustrates the tracking principle with a big SS, while Fig. 12 (B) demonstrates tracking with a small SS. The SP&O-MPE algorithm may also fail to track

Fig. 11. The P&O-MPE algorithm block diagram.
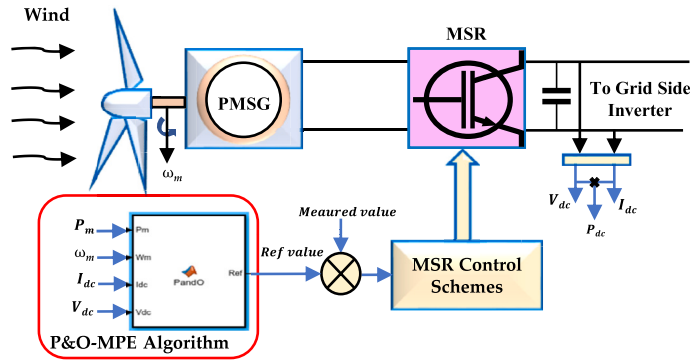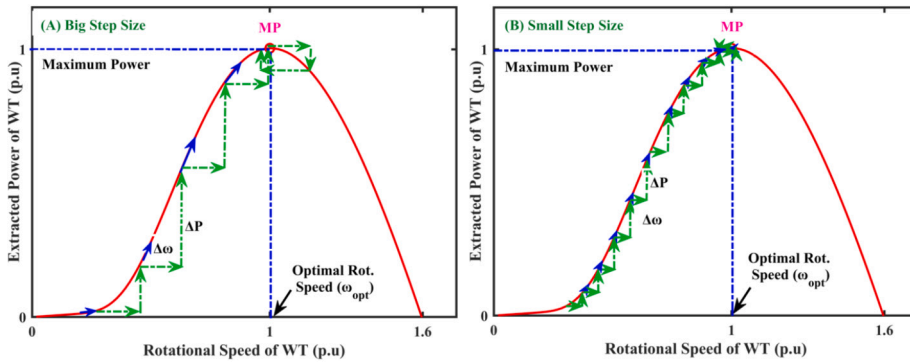

Fig. 12. The tracking principle of SP&O-MPEA (A) small SS and (B) big SS.

the optimal operating point during rapid changes in wind speed in addition to oscillations issues [110]. Therefore, the amended P&O-MPEA has been developed to address these issues [111].

5.7. AP&O-MPE algorithm

To alleviate the drawbacks of SP&O-MPEA and to enhance their tracking efficiency, researchers have proposed several AP&O-MPE [112,27,113–116,25]. The amendment in standard P&O algorithm concerns modifications in the tracking strategy via using varied SS instead of fixed SS [117]. There are three types of SSs used in the AP&O-MPE algorithm namely Variable SS, adaptive SS and hybrid SS [25]. The AP&O-MPEA of variable SS uses an SS of variable amplitude for each certain region on the WT output power curve [62], while, in the AP&O-MPEA of adaptive SS, the perturbing SS is altered adaptively at each operational point according to the main objective function [118] as shown in Fig. 13. However, the AP&O-MPEA of hybrid SS uses multiple SSs during optimal operation tracking procedure [119]. Fig. 13 (A) illustrates the tracking principle of AP&O-MPEA with variable SS, while Fig. 13 (B) shows the use of adaptive SS.

In [120,73], an AP&O-MPEA of two operation modes; namely normal P&O mode, and prediction mode was proposed. When the wind speed changes slowly, the normal P&O mode is used, while during quick changes in the wind speed, both modes are applied. In [121], an AP&O-MPE algorithm with a large forward step and a small reverse step has been introduced to overcome the slow speed of convergence of conventional P&O. Despite the enhancement in the tracking speed, a high oscillation has been experienced around the MP due to the application of large forward fixed-step. In addition anemometers were deployed to measure wind speed, which increase the cost of implementation. Likewise, AP&O-MPEA was developed in [122,123] to specify a suitable SS and direction of the next perturbing based on the distance between the operating point and the MP on the optimal curve as well as the precise value of k_{opt}. This algorithm offers a fast and efficient tracking technique; however, it sometimes tracks the MP wrongly due to the need to calculate the k_{opt} value at each wind speed.

Accordingly, the recent AP&O-MPE algorithms have been labeled into four main classes based on the general objective function, optimization strategies, division of the power curve, and hybrid approaches. The power-curve division approach typically segments the curve into numerous zones and each zone has its own controllable SS [124,27,25]. The number of operating zones and the fragmentation of the power curve affect how the algorithm handles adaptive, hybrid, or variable SSs. The power curve division framework can be identified with the aid of a synthesized curve, ratio, or relations. In [125,110], the power speed curve has been segmented into multiple zones, and anemometers are used to create a synthesized curve of four operating regions, each with a unique SS. However, this approach necessitates wind speed sensors and has an obvious transient overshoot due to the limited number of
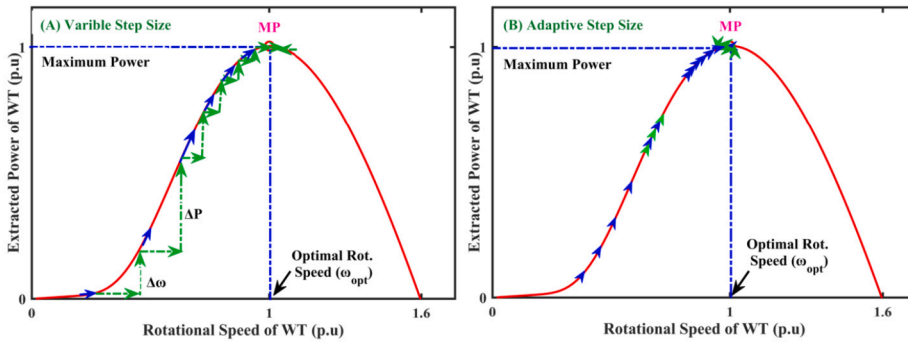
Fig. 13. The tracking principle of AP&O-MPEA, (A) Variable SS (B) Adaptive SS.

operating regions. To alleviate these constraints, the number of operating regions is expanded using adaptive SSs and flexible region boundaries in the synthesized curve, which in turn increases the complexity. The sophistication of the synthesized curve is minimized by utilizing the synthesized ratio, which comprises monitoring changes in wind turbine output power, turbine rotational speed, or both. In this regard, the authors in [62,126], used the estimated optimal power curve so as to identify the synthesized ratio.

Alternatively, the synthesized relations strategy employs control variables data, such as current, voltage, WT output power, or perturbing SSs, to establish general relationships that can be used to divide the main power curve into multiple operating regions. The specific conditions are utilized instead of the lookup table in [127,128]. In [129], two control modes with intermediary variables have been confirmed. Furthermore, other strategies in [130] employ three control modes that involve wind speed measuring and predetermined tolerance. In this context, the system complexity and the need for precise tuning of several parameters are two drawbacks to the power curve division strategy. Differently from the aforementioned algorithm, a novel sensor-less MPE based on the parabolic prediction technique (PPT) has been developed to effectively address the limitations of SP&O-MPEA and the complexities of AP&O-MPEA [131]. This PPT-MPEA was inspired by the observation that the $(P - \omega)$ curve of the WT has a parabolic shape, with a single MP for each wind speed [132–134]. Accordingly, the techniques that are utilised to locate a parabolic curve's vertex can also be utilised to locate the MP of the WT. The performance of the PPT-MPE algorithm is evaluated under different scenarios and the obtained results are compared to those of SP&O and VP&O methods. The simulation outcomes substantiate that the PPT-MPE algorithm surpassed the alternative algorithms in terms of tracking effectiveness and completely eliminating oscillation issues. This, in turn, can be considered an effective means of enhancing the VSWT system.

5.8. Smart-MPE algorithm

Aside from the aforementioned algorithms, smart approaches such as Fuzzy Logic Control (FLC) and Artificial Neural Network (ANN) based MPE algorithms play a critical role in maximizing captured wind power since these approaches do not require any arithmetic model of the systems and are not affected by changes in system parameters [102]. The FLC has been used in many MPE approaches and it generally has three main components termed fuzzification, inference engine, and defuzzification as shown in Fig. 14. The fuzzification component converts the real input values into a linguistic variable based on a membership function using seven fuzzy subsets, five subsets or other weight subsets which depend on the expert knowledge of the designer [96,135]. In the inference engine component, FLC calculates the linguistic variable in the rule inferences and then stores it in the rule table. Consequently, the defuzzification component converts the linguistic variable into real output values depending on membership functions. The input parameters of the fuzzification stage in FLC-MPEA are typically rotational speed, output power, torque variation, and/or any combination of these parameters. The output parameter is usually a reference signal which can be either torque, speed, power or duty cycle which helps to identify the optimal operating point via MSR control schemes. The FLC-MPEA has the advantages
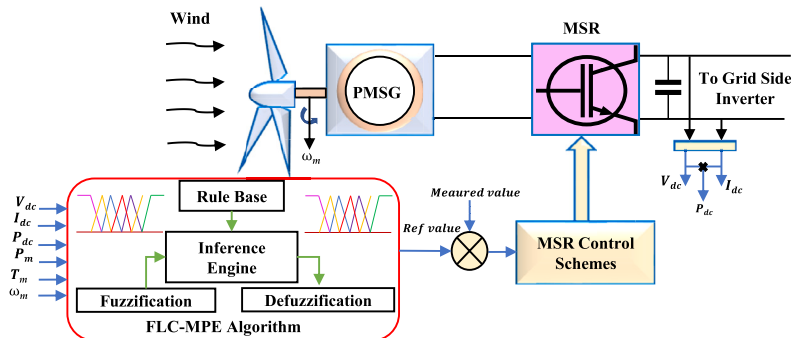

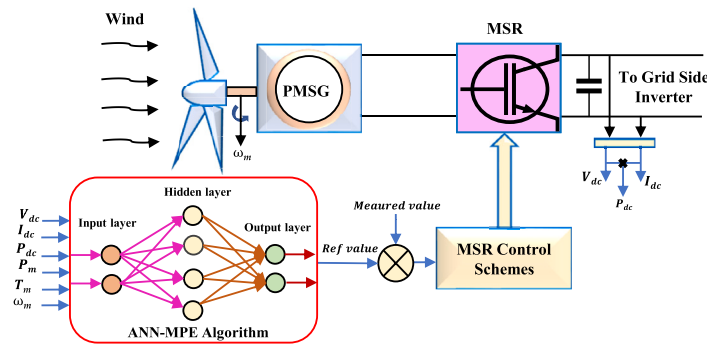**Fig. 14.** Block diagram of FLC- MPEA for VSWT system.

Fig. 15. Block diagram of ANN-MPEA for VSWT system.

of parameter insensitivity, acceptance of noisy and inaccurate signals, fast response to the dynamics system variations, and robust performance when weather patterns change [136]. Nevertheless, their performance is highly dependent on the user's knowledge of the membership function levels, choosing the rule base and selecting the appropriate error. Furthermore, the implementation of the FLC-MPE algorithm is constrained by the necessary memory requirement [137–140]. Similar to FLC, the ANN as a basis of the MPE algorithm for WECS has been implemented in many studies [31,141]. The architecture of an ANN consists of three layers: input, hidden, and output layers and the number of nodes in each layer varies and is user-dependent [142,143]. In the application of ANN for MPEA, the input variables can be terminal output voltage, torque, wind speed, rotor speed, etc. or any combination of these variables. The output variables are generally reference signals like reference power, rotor speed, torque or duty cycle as shown in Figs. 15. This reference signal consequently is provided to the MSR controller which in turn drives the power converter of the wind turbine to operate at the optimal operating point. ANN-MPEA can be quite effective and robust only after it is sufficiently offline trained for all kinds of operating conditions [144]. Nevertheless, the long offline training requires wind speed sensors, and generator rotating speed sensors which make ANN-based MPE algorithm unattractive for real-time practical in WECSs applications [21,145]. Although FLC-MPEA and ANN-MPEA are capable of beating the uncertain problem inputs and variable system parameters, their optimal response to control variables is not precisely accurate [146,147].

5.9. Hybrid-MPE algorithm

One efficacious and simple solution to overcome the weaknesses of the traditional MPEA is via the hybridization of two or more MPE algorithms. In such a hybridization the attributes of one technique are used to eliminate some drawbacks of the other technique. Numerous hybrid MPE techniques have been conducted in the literature [148,149]. In [62], [73], the OTC was merged with the P&O to solve the problems oscillation associated with the conventional P&O [150,151]. Another solution for the issues of the conventional P&O algorithm was developed in [152] by merging the P&O and PSF algorithms. On the other hand, some problems related to conventional algorithms have been solved by combining them with artificial intelligence algorithms [153]. A neural network was used together with TSR and OTC algorithm to improve their efficiency and adaptability [154,155]. An FLC approach is used to obtain an optimal SS for a conventional P&O algorithm in [156]. Overall, it may be said, that there are some difficulties in choosing the appropriate MPE algorithm for a given wind turbine system. However, based on the literature [27,124,25], as well as the discussions provided in this section, the main aspects of being considered for selecting a particular MPE algorithm are outlined in Table 4. Moreover, Table 5 provides a summary of some relevant works on the MPE algorithm and its adaption.

Table 4
Comparing MPE algorithm attributes.

Algorithm	Wind speed	Pre-information	Tracking Speed	Complexity Level	Memory Need	Performance under random wind speed
TSR-MPEA	Required	Required	Fast	Simple	Not Needed	Fairly Good
OTC-MPEA	Not Required	Required	Fast	Simple	Not Needed	Fairly Good
PSF-MPEA	Required	Required	Fast	Simple	Needed	Fairly Good
INC-MPEA	Not Required	Not Required	Slow	Simple	Not Needed	Fairly Good
ORB-MPEA	Not Required	Not Required	Median	Simple	Not Needed	Good enough
SP&O-MPEA	Not Required	Not Required	Slow	Simple	Not Needed	Good enough
AP&O-MPEA	Depends	Depends	Fast	High	Depends	Very Good
Smart-MPEA	Depends	Required	Median	High	Needed	Very Good
Hybrid-MPEA	Depends	Not required	Fast	Moderate	Depends	Very Good

Table 5

Summary of some related research on the MPE Algorithm For WECS.

Ref &Year	Algorithm	Control Inputs	Control Variable	Validation Tools	Remarks
[157] 2015	**AP&O MPEA**	Wind speed and WT's rotor speed	Electromagnetic torque	MATLAB/ Simulink	The MPEA utilizes the generator's power to furnish a reference speed. A specific setup was needed to decide the K factor, which determines VSSs.
[158] 2015	**AP&O-MPEA**	Mechanical power and rotor speed	Electromagnetic torque	MATLAB/ Simulink	An adaptive ratio was utilized to adjust the VSS. However, the sizes of steps were determined based on the system parameters.
[159] 2016	**HBD-MPEA**	Wind speed, rotational speed, and DC-power	DC-Voltage	WECS emulator and TMS320F28335	A hybrid MPEA using P&O, TSR, and PSF computational methods. The results confirm the algorithm's effectiveness.
[160] 2016	**SP&O-MPEA**	Wind speed and Generator current.	Duty cycle	LTspice IV software Experimental/Mi-crocontroller MC68HC11A8	The optimum angular speed of the turbine is calculated using the generator's output voltage with the help of a wind speed sensor..
[161] 2016	**PSF-MPEA**	Electrical power	PWM duty ratio	MATLAB/Simulink and experimental setup	A PSF-MPEA was implemented and compared to explore how overall WECS losses affect tracking process results. The Overall MPE-based PSF yields more energy than the WT-based one.
[162] 2017	**TSR-MPEA**	Wind Speed	DC-Voltage	Lab-emulator	Following the TSR-MPEA, a discrete-time reaching-law technique was incorporated into DISMC to drive the WECS.
[163] 2017	**OTC-MPEA**	Rotational speed.	Electromagnetic torque	Bladed software	Under varied wind speeds, OTC-MPE was developed and tested. Results indicated that the OTC loses power owing to large-scale wind turbine inertia.
[91] 2017	**INC-MPEA**	DCL-voltage.	DCL-current.	MATLAB/Simulink	Based on the DCL monitoring, the INC-MPEA produces the optimal reference current for the PI to regulate the inductor current of the converter to capture the maximum power.
[45] 2018	**ORB-MPEA**	DC voltage and DC current.	Duty ratio of the PWM	MATLAB/Simulink Experimental setup	An enhanced ORB-MPEA employed the PSO to detect the peak point for a wind speed and used the recorded DCL current/voltage at that point to compute the unknown ORB coefficient.
[67] 2018	**AP&O-MPEA**	DC voltage and DC current.	Appreciate duty cycle	PSIM Software and Ardinu mwga 2560	The MSR output is monitored, and the obtained data is employed to alter the duty cycle of the boost converter. Tracking speed increases, but more assumptions are needed, reducing efficiency.
[58] 2019	**AP&O-MPEA**	Generator voltage, generator current and rotor speed	Electromagnetic torque	MATLAB/Simulink dSPACE DS110	Based on theoretical analysis, a high-gain perturbing observer strategy improves WECS efficiency in response to uncertainties and nonlinearities of system.
[164] 2019	**SP&O-MPEA**	Mechanical torque and rotor speed	Electromagnetic torque	MATLAB/Simulink	The tracking process is shortened by defining the initial optimal rotational speed near the accurate optimal point based on the projected wind speed and using an SSS to minimise oscillations.
[125] 2019	**AP&O-MPEA**	Rotor speed	Electromagnetic torque	MATLAB/ Simulink	Several proposed curves and adaptive ratios are used to achieve full adaptive SSs and modular operating zone margins. Nevertheless, it is quite complicated.
[110] 2019	**AP&O-MPEA**	Rotor speed	Electromagnetic torque	MATLAB/ Simulink	This technique primarily relies on multiplying the set SSs by an adjustable ratio, determined by monitoring the error of WT rotational speed. It reduced oscillations and increased convergence speed. However, previous knowledge of the first SS is still required.
[107] 2019	**AP&O-MPEA**	Wind speed and rotor speed	Electromagnetic torque	MATLAB/ Simulink	The WT output curve is divided into four zones and the SS for each zone is selected deploying a wind speed sensor. It improves system efficiency and oscillation but has limited operating zones with hard-to-select SSs.
[165] 2019	**AP&O-MPEA**	Rotor speed	Electromagnetic torque	MATLAB/ Simulink	The SS is calculated for each modular zone by comparing a given ratio to a pre-defined ratio depending on the difference between the actual and ideal rotational speed.
[113] 2019	**AP&O-MPEA**	Rotor speed and current/voltage of grid	Electromagnetic torque	MATLAB/ Simulink and experimental	A new inertial power-based P&O-MPE are proposed considering stored energy in the WT inertia to precisely determine the optimal operating power point.
[80] 2019	**PSF-MPEA**	Wind speed and WT rotating speed	Electromagnetic torque	Simulation tool	An improved MPE method based on reducing torque gain coefficient is presented to enhance the dynamic performance of the conventional PSF approach.
[166] 2020	**TSR-MPEA**	Wind speed and rotational speed	DC-Voltage	MATLAB/Simulink	TSR-MPEA with PI and ISMC was developed to extract the MP in a five-phase PMSG-VSWT system.

Table 5 (*continued*)

Ref &Year	Algorithm	Control Inputs	Control Variable	Validation Tools	Remarks
[167] 2020	**TSR-MPEA**	Wind speed and rotational speed	Duty Cycle	MATLAB/Simulink	TSR-MPE with PI is introduced for WECS connected to DC-Bus. The captured energy was increased by 2.89% and by 4.735% for the conducted cases. However, this work needed sensors and WT parameters.
[108] 2020	**SP&O-MPEA**	Mechanical power and rotor speed	WT rotational speed	MATLAB/Simulink	A hybrid MSR control model uses a customised P&O algorithm, a second-order SMC, and battery storage to improve the SP&O algorithm.
[168] 2020	**FLC-MPEA**	DC voltage and DC current	Duty ratio of the PWM	Matlab/Simulink and PSIM co-simulation	The maximum power is sought by adjusting the PWM rectifier, which adjusts the voltage of the PMSG until it reaches the optimum rotating speed of WT.
[119] 2020	**AP&O-MPEA**	Rotor speed	Electromagnetic torque	MATLAB/Simulink	P&O-MPE algorithms of adaptive and hybrid sectors are developed on the idea of detecting the optimal output curve and adapting the perturbing SS. A fast-tracking speed with low oscillations is achieved
[118] 2020	**AP&O-MPEA**	Rotor speed	Electromagnetic torque	MATLAB/Simulink	The ideal point was searched within 10% of the WT output power curve. Then, the optimal hypothetical circle is utilised to find the suitable SS based on the distance between the optimal and real operational points.
[169] 2020	**ANN-MPEA**	DC voltage and DC current	Optimal DC	Embedded system F28M35xx and the PIL simulation	Intelligent modular multi-layer perception predicts optimal rotating speed. Then, a simplified model computes and passes the ideal current reference to the MSRCS.
[170] 2021	**TSR-MPEA**	Wind Speed and Rotational Speed	Duty Cycle	MATLAB/Simulink	A TSR-MPEA was integrated with FLC for controlling the boost converter to stay up at the optimal value. An anemometer was used to measure wind speed.
[130] 2021	**AP&O-MPEA**	Rotational speed, mechanical power and dynamic SS.	Electromagnetic torque	MATLAB/Simulink	Using Model Reference Adaptive Control (MRAC), the study provides an adaptive MPE technique that continually updates the SS without WECS settings. The optimum SS is chosen based on detecting mechanical power fluctuations and optimizing the MRAC parameters.
[171] 2021	**AP&O-MPEA**	Rotor speed and wind speed	Electromagnetic torque	MATLAB/Simulink	The search area is reduced by estimating the ideal hypothetical generator speed location using WES. Below the hypothetical position, adaptive BSSs are involved to speed up the tracking. instead, adaptive SSS is involved.
[74] 2021	**ORB-MPEA**	Electrical output power	Reference current	PSIM Software and DSP TMS320F28377S	An ORB-MPEA for small WT is developed based on the MSR's output power characteristics with regard to the output current.
[172] 2021	**INC-MPEA**	Estimated mechanical torque and speed	Optimal duty cycle	MATLAB/Simulink	the generator's current and voltage are used to estimate the mechanical torque and speed respectively. Accordingly, the tracking procedure is done based on these mechanical variables.
[171] 2021	**ANN-MPEA**	Wind speed	Rotational speed and optimum power	ARDUINO microcontroller	ANN is utilized to estimate the reference signal for optimal WT's rotational speed. The networks were trained in real-time using a backpropagation-based incremental training mode. The real-time findings demonstrated the feasibility of the ANN-based MPEA.
[97] 2021	**HBD-MPEA**	Output current and output voltage	DC- link Voltage	Matlab/Simulink	ORB has been hybridised with Gauss map-based chaotic PSO (GM-CPSO) and chaotic dynamic weight PSO (CDW-PSO). The GM-CPSO and CDW-PSO have been employed to acquire the Kopt of the ORB. Once the Kopt is obtained, the ORB-MPE method is triggered according to the received Kopt.
[173] 2022	**OTC-MPEA**	Rotational speed	Electromagnetic torque	FAST platform	A wind speed estimator was developed to estimate the tracking error of optimal rotor speed in order to improve the acceleration and deceleration performance of conventional OTC.
[174] 2022	**ORB-MPEA**	Mechanical rotating speed	Duty ratio of the PWM	MATLAB/Simulink Experimental setup	The pre-determined look-up table of the ORB approach was based on the ideal relationship between the WT's rotating speed and the PMSG's power output which had been obtained by a model-free reinforcement learning algorithm.
[78] 2022	**OTC-MPEA**	Rotor speed and system parameter	Optimal torque	MATLAB/Simulink	OTC-MPEA and a FLC have been introduced to the MSR to enhance the overall efficiency of the studied WECS.
[93] 2022	**INC-MPEA**	Estimated optimal voltage	Optimal duty cycle	MATLAB/Simulink	INC approaches are used to figure out the optimal duty cycle based on the optimal voltage. The ANN was used first in this case to estimate the optimal voltage based on the measured wind speed and voltage output.
[175] 2022	**FLC-MPEA**	DC voltage and DC current	Duty ratio of the PWM	MATLAB/Simulink	In this work the momentary error of both DC link voltage and DC- link power have been used as input for FLC in order to generate the optimal duty cycle which extracts the maximum power for any wind speed data.

Table 5 (*continued*)

Ref &Year	Algorithm	Control Inputs	Control Variable	Validation Tools	Remarks
[176] 2022	**ANN-MPEA**	Active power and actual rotor speed	Optimal rotor speed	Matlab/Simulink and Experimental set up	A novel reinforcement Q-learning-based MPE algorithm was developed for PMVG-VSWT that relies solely on training and does not require knowledge of WT characteristics or wind speed.
[150] 2022	**HBD-MPEA**	Mechanical power and mechanical speed	duty cycle	Matlab/Simulink and Experimental set up	A hybrid MPEA based on HCS, OTC and FLC in the composition of power management systems to improve the performance of the WECS with storage batteries. The obtained finding proved the hybrid approach outperformed the others.

6. Control schemes of MSR/GSI

The FCPEC equipped with the PMSG-VSWT system is a type of power electronic converter that connects two separate electrical systems of different voltages/frequencies. It is essentially two converters namely MSR and GSI connected back to back via a DC-link capacitor [177–180]. These MSR/GSI involve a complex system that necessitates enhanced control schemes for power quality and stability while maximising conversion efficiency [181–187]. In this topology, the MSRCS controls the power flow from the PMSG and ensures that the WT operates at its optimal rotational speed [165,188]. While, the GSICS achieves decoupled control of active and reactive power injected into the grid, maintaining consistent DC-link and grid line voltages, and improving overall system performance [189,190] [191]. The common control schemes used for controlling the MSR/GSI of FCPECs integrated with PMSG-VSWT are based on FOC/VOC, DTC/DPC, MPC and SMC [192–195]. The following subsection discusses, the working principle, pros and cons, and some related work of these common control approaches.

6.1. SMC-based MSR/GSI control schemes

Slide mode control (SMC) is a robust control method that uses a sliding mode surface to maintain the system behavior close to the desired trajectory, by designing a control law that ensures the system state remains on a sliding surface defined as the difference between the actual and desired states. SMC method has received a lot of attention as one of the control approaches in both linear and nonlinear systems due to its robustness, insensitivity to parameter variations, finite-time convergence, disturbance rejection, and good dynamic behavior. In the domain of WECS control, numerous studies with various control objectives for the PMSG-VSWT system have been conducted employing SMC-based MSR/GSI control schemes. The general block diagram of SMC-based MSR/GSI for the VSWT system is described in Fig. 16. In the context of SMC applications, study [196], presented a conventional SMC for PMSG-VSWT to ensure the GSI's stable operation in an HVDC station during DC faults. The same issue was addressed in [197] by adopting a generalized high-order disturbance observer with integral SMC (ISMC). In the provided study, a disturbance observer was used to estimate rapidly changing uncertainty, while rotor speed regulation was handled by the ISMC. However, the chattering phenomenon, which is caused by the standard SMC's discontinuous function, is the most significant shortcoming of this control scheme. Hence, many strategies have been introduced to eradicate or attenuate the chattering issue which negatively impacts the SMC controller's robust performance and is undesirable in the WECS [198]. One of the fascinating ways for reducing chattering is to employ adaptable reaching law rather than regular reaching law [199]. In articles [200], an enhanced exponential RL-based SMC was presented and investigated to reduce the chattering issue and improve the total harmonic distortion properties of WECS. The obtained output demonstrated chattering mitigation and VSWT system transient improvements. Another way to improve SMC is introducing the fractional order (FO) SMC that outperforms its integer counterpart in control performance due to more adjustable parameters and the memory effect introduced by FO differential operators. This leads to reaching equilibrium with faster convergence [201,202]. In [203] a nonlinear FO-SMC scheme was suggested to enhance the quality of power production. Comparative studies with SMC showed that the suggested nonlinear FO sliding surface with differentiation components and fractional integration minimized chattering and produced more power than conventional SMC and PI. Besides, Authors in [204] came up with two GSA-optimized FO-SMC strategies to control MSR/GSI in order to improve turbine output power quality. Although the proposed control technique has improved tracking accuracy and was more robust against parametric disturbances, there was still some slight chattering.
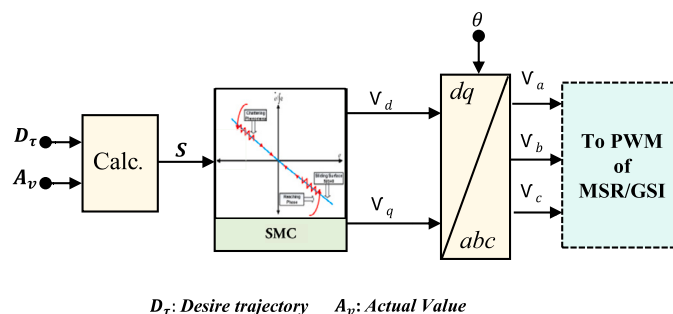

D_τ: *Desire trajectory* A_v: *Actual Value*

Fig. 16. Block diagram of SMC-based MSR/GSI control.

An alternative option to reduce the chattering is utilizing the Higher-order SMCs (HO-SMCs) that take HO derivatives into account concerning time. The HO sliding variable and its subsequent derivatives converge to zero in finite time with improved stabilization precision resulting in reducing the undesirable consequences of the chattering phenomena and hence the control system becomes much more resilient to uncertainties and disturbances [205–207]. The most of HO-SMCs applied in PMSG-VSWT are the second-order SMC(SO-SMC), the super-twisting SMC (ST-SMC) and the terminal SMC (T-SMC) [208–210]. In [211], an experimental study of a control strategy based on a SO-SMC and the disturbed single input– single output error model was proposed to control the MSR/GSI of a real-time VSWT simulator. The authors claim that the devised control technique effectively controlled the speed turbine generator and DC-link voltage in the presence of unknown disturbances, parametric variation, and uncertainties since the presented SO sliding surface effectively reduced chattering. In [212], a two-stage cascade-structured control strategy for a large-scale PMSG-VSWT connected to the grid was performed. The scholars developed a SO-SMC control system that effectively minimized the resistive losses into the generator and controlled the active and reactive powers transmitted to the grid. The developed scheme's ability to withstand external troubles unmodeled dynamics and 3-phase voltage descents was evaluated in this study. As stated, the developed control system ensured convergence in finite time and reduced chattering. In [213] the authors presented two T-SMC controls of reduced chattering to control the active and reactive powers transferred between the GSI and the UG. In this work, the chattering was reduced via utilizing integrators which in turn provide continuous control signals and smooth out switching signals. The effectiveness of the presented control scheme in terms of reducing control energy wastage and resilience against matched as well as mismatched parametric uncertainties was established. In [214], the authors developed and implemented a composite SMC of a soft-switching sliding-mode observer (SS-SMO) and a non-singular (NTSMC). The SS-SMO is used to observe the disturbances, whereas the NTSMC is used as a speed controller. The chattering problem was settled by replacing the traditional signum switching function in the disturbance observer loop with the smooth hyperbolic tangent function. This methodology is strong against model uncertainty and exterior disturbances. It also makes the system simpler by replacing mechanical speed and position sensors with parameter estimation. Although the proposed ways to reduce the chattering phenomenon of SMC can be effective, they also add complexity to the overall design and implementation as well as require complex calculations and computations. This can place a heavy burden on the control system's hardware and software resources, increase the chances of design errors, and make it difficult to achieve robust performance. In addition, the HO-SMC systems are even more sensitive to variations in system parameters than lower-order systems. This can make it difficult to achieve robust performance in systems with uncertain or changing parameters. Table 6 summarises some work related to MSC-based MSR/GSI control schemes.

Table 6
Summary of some relevant work on SMC Based MSR/GSI Control systems.

Year	Ref	Strategy	The goal of control	Remark
2015	[212]	SO-SMC	Controlling the delivered active and reactive power to the grid	Chattering is minimized by utilizing SO-SMC. Unmodeled dynamics as well as external perturbations are taken into account. However, chattering mitigation is not properly addressed, and no comparisons were provided.
2016	[211]	ST-SMC	Turbine speed controlling and DC-link regulation	Chattering is minimized by utilizing ST-SMC and parametric uncertainties while external troubles were considered. However, the chattering was not fully looked into, and no comparisons were given.
2017	[215]	C-SMC	Regulating the speed of the WT as well as the grid's current and voltage.	The control mechanism was designed to reduce chattering and overshoot with minimum settling time. However, the delivered results have not revealed their significance and no comparison was provided.
2018	[216]	C-SMC	Eliminating asymmetrical voltage sags' effects at common coupling point and suppressing disturbances' effects	In this work, the asymmetrical voltage sag problems are addressed individually by decoupling control of the DC voltage and both active/reactive power (AP/RAP). The designed approach allows the WT to remain connected to the grid and provide AP/RAP support during voltage dip sags. The chattering was not addressed.
2019	[217]	C-SMC	Enhancing the system's maximum power extraction performance	This work introduced an extended state observer into the architecture of the SMC, which substantially decreases chattering and improves the method's practicality. Nevertheless, the issue of chattering was not adequately addressed and external troubles have not been considered.
2020	[204]	FO-SMC	Controlling the DC-link and grid voltage, as well as regulating the output AP and RAP of the WT.	Chattering is diminished by utilizing adaptive FO-SMC while considering external troubles. However, the issue of chattering was not adequately handled compared to other SMC.
2021	[201]	FO-SMC	Controlling speed for maximum power extraction.	Chattering is reduced by employing the FO-SMC. However, external disturbances were not considered and the issue of chattering was not fully solved.
2022	[195]	SO-SMC	Maximum power extraction and smoothing injected power.	SO-SMC with an adaptive-gain super-twisting algorithm is proposed to ensure power injection into the grid is smooth and eliminates the chattering effect compared to the traditional SMC. However, external disturbances were not considered

6.2. MPC-based MSR/GSI control schemes

Model Predictive Control (MPC) is a set of predictive control techniques that predict the future behavior of the system under control based on a model of the system and a time horizon. The system usually runs an online optimization procedure to find the best course of action for controlling the system so that the predicted output equals the reference value. Existing MPC approaches for PEC are indexed into two sets: MPC of finite control set (FCS-MPC) and MPC of continuous control set (CCS-MPC) [218,219]. The
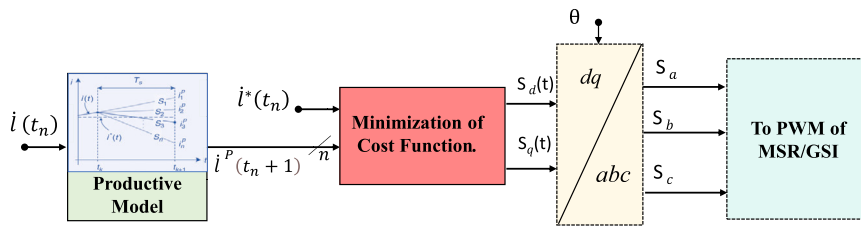
Fig. 17. Block diagram of MPC-based MSR/GSI control schemes.

FCS-MPC is based on the discrete behavior of converters and so eliminates the use of PWM regulators, unlike the CCS-MPC which is based on generating continuous signals to drive converters via the PWM regulator. The general topology of MPC for Controlling PEC is shown in Fig. 17. The MPC has been widely utilised in the last years for controlling FCPEC integrated with wind energy conversion systems due to its merits of controlling flexibility and robustness. In [220], authors presented an MPC-based control scheme to control active and reactive power at the turbine and grid terminal via internal current loop controllers. The designed MPC schemes estimate the future behavior of the system throughout each sampling interval using a mathematical model. Then a predetermined cost function is used to optimize the switching signal combination. The outcome showed that the MPC-based controller features high transient dynamic and low THD grid current. In [221], the MPC strategy with a finite control set has been introduced for controlling MSR to achieve the optimal turbine rotating speed. In this study, the nonlinear model of WT is linearized using data from an unconventional extended Kalman filter. The optimal generator speed tracking error and the cost of the torque actuation act at the MPE region were both evaluated using a quality function. The findings show that the suggested MPC is efficient for optimum speed maintenance and producing a quick dynamic. Nevertheless, the presented approach model was not able to provide precise future WT behaviors in the absence of wind speed forecasting when there is a strong wind disturbance. In [222], authors developed a novel FCS-MPC intending to reduce the required calculations in each horizon and overwhelming the variable switching frequency issue in the control schemes of FCPEC of VSWT-PMSG. In this study, the performance of the suggested approach is compared with conventional FCS-MPC and the results show an improvement in the total harmonic distortion ranges and the simulation time. In article [223] a deadbeat MPC (DB-MPC) with the aid of an extended Kalman filter (EKF) is designed to reduce the harmonic distortion in the stator currents and enhance the quality dispatched power from PMSG-VSWT. In this work, the extended Kalman filter (EKF) was used to estimate the total disturbance caused by variations of the PMSG parameters which is then included in the design of the DB-PC strategy. The developed method has been validated via experimental work in the laboratory and compared with conventional techniques. The obtained results proved that the reliability of the drive system was improved and the system was much more robust to parameter variation. In [224], authors presented a new nonlinear MPC scheme for wind farm frequency regulation. The designed MPC incorporates the nonlinear dynamic behavior of each wind generator to achieve optimal frequency response and stability. The developed control scheme's performance is tested under the condition of under/over frequencies. Simulation outcomes demonstrate that, in the presence of under/over frequency circumstances, the developed approach adapts rapidly to frequency deviations, enhances frequency nadir/peak, and ensures wind turbine stability. Moreover, in [225], a new direct model predictive flux and power control for both MSR and GSI with reduced computational cost and enhanced control performance was developed to improve the power quality injected into the grid and to comply with grid codes. Extensive experimental work is used to assess the performance of the proposed control strategies and establish their validity. The experimental outcomes proved that the presented methodology performed lower THD values for PMSG and grid, and indicated significant robustness against the parameter deviations, confirming that the investigated mechanisms are a more feasible and effective option for PMSG drives. Many other MPCs approaches have been developed for maximum power extraction, grid voltage and frequency regulation, active and receive power control, grid power quality, and fault ride-through (FRT) as stated in [226–228,221,229–231].

6.3. DTC/DPC based MSR/GSI control schemes

The direct torque control/direct power control (DTC/DPC) approaches are alternatively structures used to control MSR/GSI in WECS applications. The DTC approach is primarily used to manage the MSR part and is based on a pair of hysteresis compactors and a LuT, as illustrated in Fig. 18. This strategy is interesting, especially for controlling low-power WECS. This strategy regulates the electromagnetic torque and stator flux immediately and separately [232,233]. It has the advantages of insensitivity to generator parameters variation, absence of rotor position sensors, absence of current controller, etc. Nevertheless, the high ripples, a fluctuation in the frequency of switching with rotor spinning speed, and the bandwidth of two hysteresis comparators are some drawbacks of DTC compared to FOC [234]. The irregular ripples cause over-stress on the WT rotating shaft, decrease the WT lifetime, and generate a lot of noise. An efficient way of addressing ripple issues is to incorporate space vector modulation (SVM) into the DTC [235,143,33]. An alternative approach involved incorporating observer-based adaptive speed control, demonstrating satisfactory results in solving this issue [236]

On the other hand, the DPC method is used to control the GSI component, which is identical in theory to the DTC method for MSR. In this method, the instantaneous active and reactive powers are used as two control variables while both of PWM modulator circuit and current control system loop are eliminated as seen in Fig. 19 [237,32]. Instead, the switching states are determined using a LuT. A unity-power-factor operational mode in the DPC method is typically accomplished by keeping the reference of reactive
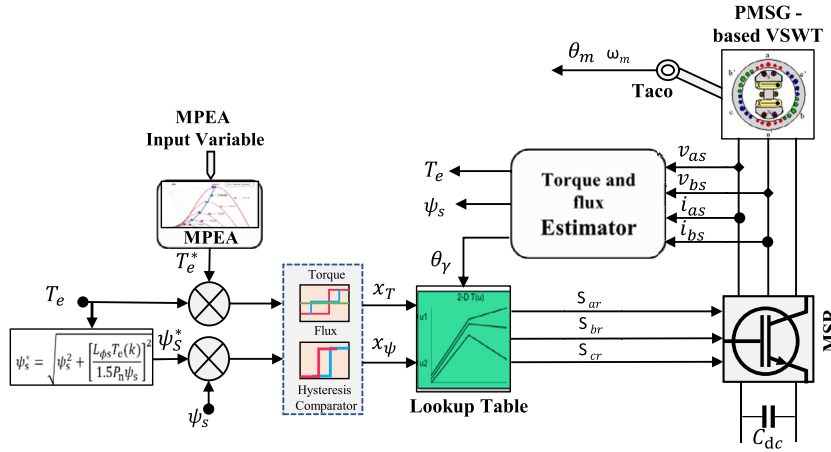
Fig. 18. Block diagram of DTC control schemes of MSR.
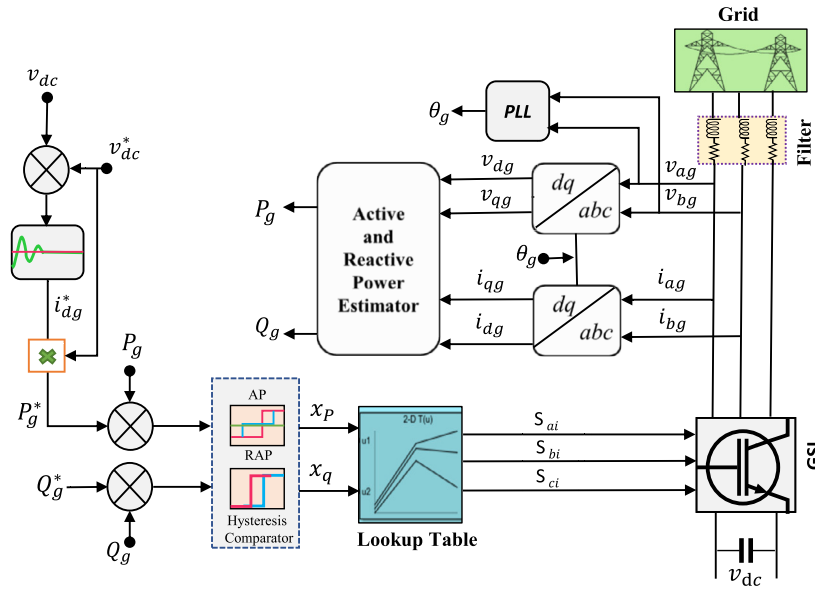
Fig. 19. Block diagram of DPC control schemes of GSI.

power at zero. The DPC has the advantages of simple implementation, the absence of the active-reactive power cross-coupling effect, fast dynamic response, and high robustness to parameter variations [192,238,225,239]. However, Considerable power quality issues of THD and power/current ripple are significant DPC flaws. Moreover, the DPC requires a high filter inductance due to the variable switching frequency in addition to a high sampling because of the rapidly changing estimated active and reactive powers. The issue of ripple in DPC can be effectively mitigated by integrating Space Vector Modulation into the DPC framework. This integration has been shown to result in a significant reduction in Total Harmonic Distortion (THD) and the maintenance of a consistent switching frequency, as evidenced by the research of Tiwari et al. [21], Liu et al. [240], and Zoghlami et al. [241].

Similarly, enhancing power quality has been achieved by introducing a third-order signal integrator-based control technique [49], alongside a multi-layer, frequency adaptive fundamental signal extractor-based filter [17], and a multistage adaptive filter [236]. These methods have demonstrated substantial effectiveness in mitigating THD, as observed through experimental results. Furthermore, their efficiency has been proven under a wide range of dynamic conditions, underscoring their versatility and reliability in various power system scenarios.

6.4. FOC/VOC based MSR/GSI control schemes

The cascaded vector control-based field-oriented control/voltage-oriented control(FOC/VOC) is the most dominant strategy investigated for controlling MSR/GSI in WECS applications as they provide a higher level of precision and accuracy in controlling the power output of the turbine and better performance for grid integration [242]. This is because both of them use a vector control
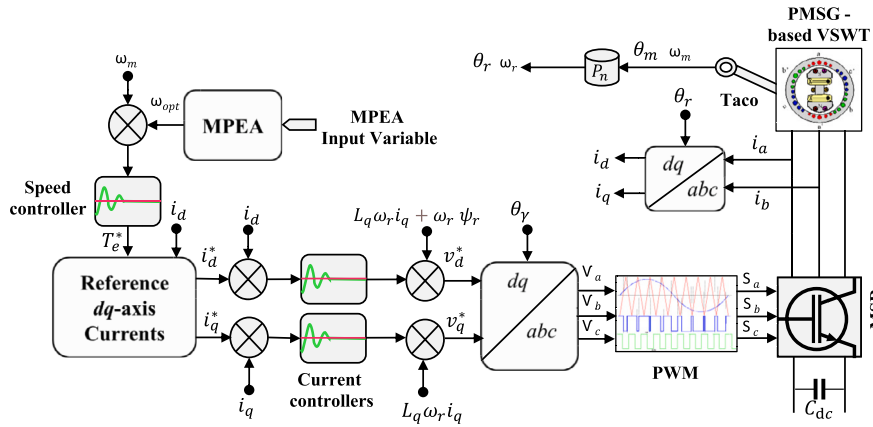
Fig. 20. Block diagram of FOC control schemes of MSR.
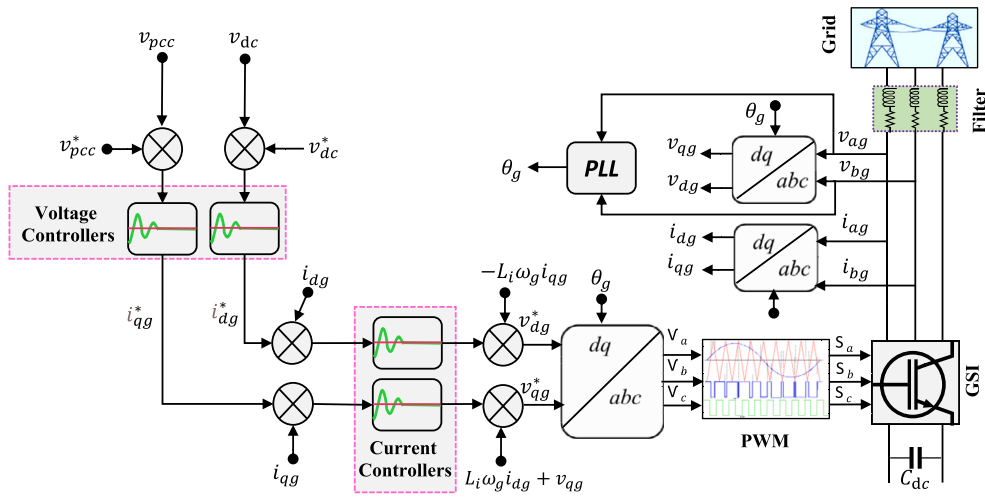
Fig. 21. Block diagram of VOC control schemes of GSI.

approach that takes into account the phase relationship between the voltage and current, and the rotor position of the turbine's generator which in turn, enables more accurate control of the power electronic converter [243–245]. In the FOC/VOC strategy, the FOC is used for controlling the MSR part, while the VOC serves to control the GSI part. The FOC utilizes a dual-loop control structure, consisting of an outer loop for controlling the speed and an inner loop for controlling the current as shown in Fig. 20. The outer control loop is used for the WT speed controlling as well as achieving peak electromagnetic torque/amp and zero d-axis currents. Whilst in the inner control loop, the torque is regulated by the q-axis stator current, and the d-axis stator current is constrained to be zero.

On the other side, the VOC is in charge of controlling the GSI to ensure that the power generated by the wind turbine is properly synchronized with the UG and the power quality meets the requirements set by the grid operator including maintaining voltage/frequency stability and power flow. The VOC mechanism is similar to the FOC in that it uses a dual-loop control structure, with an internal current regulator loop and an exterior terminal voltage and Dc-link voltages controller loop as shown in Fig. 21. Where the active and reactive powers are controlled by regulating the dq-axis grid currents and a unity-power-factor operations mode can be reached by setting the q-axis current reference to zero [33,210,246]. Since the current is regulated directly in this scheme, the output currents have minimal harmonic distortion, leading to valuable efficiency. However, the performance still heavily depends on the modulation type and the kind of applied controller. [33,192,183,185]. According to published works on MSR/GSI control schemes, the cascaded vector control VOC/FOC is mainly implemented using a proportional-integral control (PIC), sliding mode control, model predictive control, adaptive control, artificial intelligent control or a combination of these techniques [247,29,248, 249]. However, PIC is still prevalent in many industrial applications owing to its characteristics, such as simplicity, sturdiness, and broad stability ranges. [250]. Nonetheless, PIC is extremely vulnerable to uncertainty, non-linearity, and parameter variations of the system [251]. As a result, numerous ways for appropriately designing cascaded PIC gains have been presented in the literature [252]. Most of those ways depended on error and trial standards for developing such a controller, which is time-consuming, requires considerable effort, and is largely dependent on the designer's skill. Consequently, fine-tuning PIC presents a crucial challenge to

Table 7
Summary of the implemented approaches based-FOC/VOC control systems for MSR/GSI.

Year	Ref	Controller	The goal of control	Remark
2018	[268]	ANFIS-GA	Enhancing the grid-tied VSWT performance at a fault scenario.	GA was introduced to identify the ANFIS parameters which are in charge of controlling both MSR and GSI for achieving good performance.
2019	[269]	MPC & PIC	MPE, Dc-link voltage regulation and injection power of UPF.	The MPC is utilized to alter the rotor's speed relative to its reference speed given by the MPE algorithm. while the cascaded PI controllers were applied to control the dq-axis current and Dc-link voltage of GSI.
2020	[252]	Self-tuned PIC	Improving the power grid-tied VSWT behavior.	This work introduced a cascaded self-tuned PICs scheme to effectively control both the MSR/GSI. The gains of the multiple cascaded PIC were continuously updated employing the IMSAF technology.
2021	[262]	Optimized PIC	MPE, regulating the V_{DCL}, and keeping V_{PCC} constant.	The SCA was developed to optimally design the PIC gains based on six PIC's error inputs during the simulation model running. The obtained results proved that SCA was able to reduce the controller error resulting in enhanced performance.
2021	[270]	Adaptive PIC	MPE and enhance fault ride-through capability.	Adaptive filtering algorithm named the least mean the square root of the exponential algorithm is applied to self-tune the gains of the cascaded PIC-based MSR/GSI control schemes.
2022	[271]	PIC	Controlling DC-link voltage for power smoothing improvement	In this work, seven PICs were used to control MSR/GSI in a cascaded structure. However, the work concentrated on developing an improved time DC-link voltage control technique based on a low-pass filter. The transfer function is used to determine proper parameters.
2023	[254]	Optimized PIC	Extracting maximum power and deliver stable power to the grid	In this work, the golden eagle optimization algorithm is used to find the best setting for eight cascaded PI controllers in the MSR/GSI. In the optimization process, the integral square error criterion was considered a fitness function.
2023	[272]	PIC & SMC	Getting stable power output from WT and regulating DC-link voltage	ISMC was used to regulate WT rotating speed and DC-Link voltage while the PICs applied to control dq-axes current for both MSR and GSI
2023	[263]	Optimized PIC	enhancing the MPE and FRT	A novel HSCATSO algorithm was used to optimal six PIC in coordination with a new MPE algorithm

control developers, especially in WECS, where mathematical models or transfer functions are challenging to obtain. Therefore, many meta-heuristic algorithms have recently been utilized to fine-tune cascaded PIC gain for enhancing PMSG-VSWT performance [253]. Among examples of the applied algorithms are the olden eagle optimization algorithm [254], augmented grey wolf optimizer [255], Gorilla tropical optimization algorithm [256], democratic joint operations algorithm [257], Grey Wolf Optimizer [248], whale optimization algorithm [258], particle swarm optimization algorithm [259], optimal transient search algorithm [260], symbiotic optimization algorithm [261], and sine cosine algorithm [262]. By utilizing the aforementioned optimization approaches, significant improvements are genuinely achieved for the PMSG-VSWT system. However, based on the NFL theorem, no particular algorithm can efficiently handle all optimization issues. Consequently, some researchers have devised a hybrid optimization algorithm aimed at improving the performance of single algorithms and then applied these algorithms to optimally design the cascaded control schemes of MSC/GSI. [263]. Alternative research works have proposed smart and passivity techniques to address the challenges associated with conventional PI controller-based vector control [264,265]. In [266], an intelligent controller that leverages passivity and fuzzy logic is introduced. This approach aims to enhance torque optimization and resolve robustness issues inherent in traditional PI controllers. The proposed method's effectiveness is demonstrated through simulations, and its practical applicability is also confirmed. Meanwhile, In [14,267], a new design for a passivity-based current controller with flux orientation is presented. This energy-based technique incorporates a damping term to ensure stability and convergence of measured signals to their reference values, thereby improving the performance of the wind system. Table 7 summarises the implemented approaches-based FOC/VOC for MSC/GSI control schemes.

7. Research trend and future direction

The research trends in the domain of MPE algorithm and MSR/GSI control schemes introduced for PEC interfacing the PMSG-VSWT systems can be seen in Fig. 22. Current research trends and technology indicate that the P&O-MPE algorithm is the most considerably researched method due to its advantages of being sensorless, requiring no prior system knowledge, and being simple. The trend also exposes that the TSR is gaining some attention due to its simplicity and robustness. Other MPE algorithms, on the other hand, have gotten varied degrees of attention due to some of the constraints. Turning to MSR/GSI control schemes, the research trend reveals a significant focus on FOC/VOC approaches, which have garnered substantial interest due to their effectiveness and accuracy. Conversely, the SMC scheme has received fair interest and is being researched in a few studies. The trend also informs that the DTC/DPC approach is mostly integrated for low-scale PMSG-VSWT systems, and earns the least attention. Overall, the research trends highlight the importance of developing effective control strategies, improving MPE algorithms, and addressing grid-interconnection challenges in PMSG-based VSWT systems. On the other hand, the future direction of control technologies for this FCPEC is expected to focus on approaches that enable the converter to operate in both grid-forming and grid-following modes in response to the increasing adoption of renewable energy grids. These approaches may involve integrating machine learning and multi-objective optimization techniques. Machine learning can produce accurate MPEA and responsive control schemes. Whereas
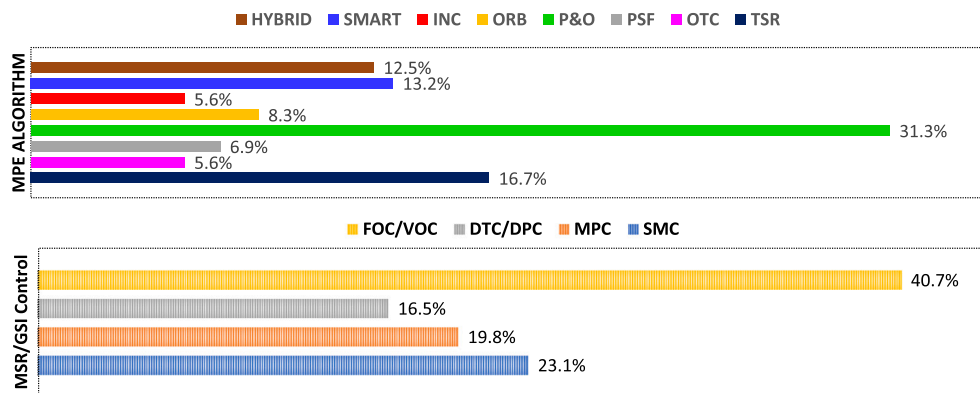
Fig. 22. Research trends of control approaches established for PMSG-VSWT system.

multi-objective optimization approaches are valuable for ensuring a well-balanced approach that considers objectives of maximum power capturing, grid stability, and power quality.

8. Conclusion

The efficient use of wind energy is becoming increasingly imperative, leading to a rise in interest in VSWT systems with power electronic interfaces among turbine manufacturers. The PMSG coupled with FCPEC is gaining popularity in VSWTs due to its fully controllable operation which enhances wind power harnessing and the quality of grid wind power integration. The primary control schemes associated with FCPEC, including the MPE algorithm, MSR control scheme, and GSI control schemes, play a crucial role in achieving control objectives. Therefore, various approaches based on these schemes are proposed in the literature for this purpose. In this article, the MPE algorithms and MSR/GSI control schemes used for FCPEC within the grid-tied PMSG-VSWT system were comprehensively and systematically reviewed. The focus was on elucidating their working principles, merits and demerits, control objectives, and recent related work. A thorough analysis of the MPE algorithm proves valuable for researchers in choosing the most suitable method for their specific work. It also provides a pathway to tackle unresolved limitations and challenges. These insights serve as valuable guidance, inspiring further exploration and enhancements in the domain of MPE algorithms. Given the MSR/GSI control schemes, the article critically analyzes the approaches that have been proposed as the basis of these schemes, such as FOC/VOC, DTC/DPC, SMC, MPC, optimization algorithms, and other modern techniques. It extensively investigates these schemes, focusing on recent progress, improvements, and modifications. The article also details the issues and challenges associated with these approaches. Furthermore, it states existing control strategies can be further refined to achieve faster and more optimal control performance. Upon examining the current technology trends and the status of research aimed at achieving optimal WECS, it is anticipated that future studies will focus on advancing existing control strategies. These advancements are expected to leverage machine learning and multi-objective optimization techniques to further enhance the effectiveness. This review is projected to be a useful resource for researchers in the area of grid-integrated PMSG-based VSWT systems.

CRediT authorship contribution statement

Hussein Shutari: Writing – review & editing, Writing – original draft, Methodology, Formal analysis, Conceptualization. **Taib Ibrahim:** Writing – review & editing, Visualization, Supervision. **Nursyarizal Bin Mohd Nor:** Writing – review & editing, Visualization, Supervision. **Yahya Z. Alharthi:** Writing – review & editing, Visualization, Funding acquisition. **Hakim Abdulrab:** Writing – review & editing, Visualization.

Declaration of competing interest

The authors declare that they have no known competing financial interests or personal relationships that could have appeared to influence the work reported in this paper.

Data availability statement

No additional data is associated with this paper.

Acknowledgement

References

[1] W. Zheng, P.P. Walsh, Economic growth, urbanization and energy consumption—a provincial level analysis of China, Energy Econ. 80 (2019) 153–162, https://doi.org/10.1016/j.eneco.2019.01.004.

[2] G. Semieniuk, L. Taylor, A. Rezai, D.K. Foley, Plausible energy demand patterns in a growing global economy with climate policy, Nat. Clim. Change 11 (4) (2021) 313–318, https://doi.org/10.1038/s41558-020-00975-7.

[3] M. Elheddad, C. Benjasak, R. Deljavan, M. Alharthi, J.M. Almabrok, The effect of the fourth industrial revolution on the environment: the relationship between electronic finance and pollution in oecd countries, Technol. Forecast. Soc. Change 163 (2021) 120485, https://doi.org/10.1016/j.techfore.2020.120485.

[4] Q. Jiang, Z.U. Rahman, X. Zhang, M.S. Islam, An assessment of the effect of green innovation, income, and energy use on consumption-based co2 emissions: empirical evidence from emerging nations brics, J. Clean. Prod. 365 (2022) 132636, https://doi.org/10.1016/j.jclepro.2022.132636.

[5] S. Dyatlov, N. Didenko, E. Ivanova, E. Soshneva, S. Kulik, Prospects for alternative energy sources in global energy sector, IOP Conf. Ser. Earth Environ. Sci. 434 (2020) 012014, https://doi.org/10.1088/1755-1315/434/1/012014.

[6] M. Majid, et al., Renewable energy for sustainable development in India: current status, future prospects, challenges, employment, and investment opportunities, Energy, Sustain. Soc. 10 (1) (2020) 1–36, https://doi.org/10.1186/s13705-019-0232-1.

[7] D. Bogdanov, A. Gulagi, M. Fasihi, C. Breyer, Full energy sector transition towards 100% renewable energy supply: integrating power, heat, transport and industry sectors including desalination, Appl. Energy 283 (2021) 116273, https://doi.org/10.1016/j.apenergy.2020.116273.

[8] U. Mehmood, Contribution of renewable energy towards environmental quality: the role of education to achieve sustainable development goals in g11 countries, Renew. Energy 178 (2021) 600–607, https://doi.org/10.1016/j.renene.2021.06.118.

[9] D. Bogdanov, M. Ram, A. Aghahosseini, A. Gulagi, A.S. Oyewo, M. Child, U. Caldera, K. Sadovskaia, J. Farfan, L.D.S.N.S. Barbosa, et al., Low-cost renewable electricity as the key driver of the global energy transition towards sustainability, Energy 227 (2021) 120467, https://doi.org/10.1016/j.energy.2021.120467.

[10] D. Alemzero, T. Acheampong, S. Huaping, Prospects of wind energy deployment in Africa: technical and economic analysis, Renew. Energy 179 (2021) 652–666, https://doi.org/10.1016/j.renene.2021.07.021.

[11] statista, Projected global cumulative wind power capacity from 2017 to 2022, https://www.statista.com/statistics/185551/global-wind-market-forecast-by-cumulative-capacity-since-2010/. (Accessed 21 June 2021).

[12] Global Wind Energy Council, Global wind report 2021, https://gwec.net/global-wind-report-2021/. (Accessed 11 July 2021).

[13] M. Hannan, A.Q. Al-Shetwi, M. Mollik, P.J. Ker, M. Mannan, M. Mansor, H.M. Al-Masri, T.I. Mahlia, Wind energy conversions, controls, and applications: a review for sustainable technologies and directions, Sustainability 15 (5) (2023) 3986, https://doi.org/10.3390/su15053986.

[14] Y. Belkhier, A. Achour, N. Ullah, R.N. Shaw, Modified passivity-based current controller design of permanent magnet synchronous generator for wind conversion system, Int. J. Model. Simul. 42 (2) (2022) 192–202, https://doi.org/10.1080/02286203.2020.1858226.

[15] M. Zribi, M. Alrifai, M. Rayan, Sliding mode control of a variable-speed wind energy conversion system using a squirrel cage induction generator, Energies 10 (5) (2017) 604, https://doi.org/10.3390/en10050604.

[16] K. Sabzevari, N. Khosravi, M. Bakr Abdelghany, Y. Belkhier, M. Tostado-Véliz, H. Kotb, S. Govender, Low-voltage ride-through capability in a dfig using fo-pid and rco techniques under symmetrical and asymmetrical faults, Sci. Rep. 13 (1) (2023) 17534, https://doi.org/10.1038/s41598-023-44332-y.

[17] T.N. Gupta, S. Murshid, B. Singh, Improving power quality of single phase utility grid connected to wind–pv system using multilayer-frequency adaptive fundamental signal extractor, IET Renew. Power Gener. 14 (12) (2020) 2126–2134, https://doi.org/10.1049/iet-rpg.2019.0928.

[18] A. Mansouri, A. El Magri, R. Lajouad, I. El Myasse, F. Giri, et al., Wind energy based conversion topologies and maximum power point tracking: a comprehensive review and analysis, e-prime-advances in electrical engineering, Electron. Energy (2023) 100351, https://doi.org/10.1016/j.prime.2023.100351.

[19] A. Mansouri, A. El Magri, R. Lajouad, F. Giri, Control design and multimode power management of wecs connected to hvdc transmission line through a Vienna rectifier, Int. J. Electr. Power Energy Syst. 155 (2024) 109563, https://doi.org/10.1016/j.ijepes.2023.109563.

[20] F. Blaabjerg, K. Ma, Wind energy systems, Proc. IEEE 105 (11) (2017) 2116–2131, https://doi.org/10.1109/JPROC.2017.2695485.

[21] R. Tiwari, N.R. Babu, S. Padmanaban, L. Martirano, P. Siano, Coordinated dtc and voc control for pmsg based grid connected wind energy conversion system, in: 2017 IEEE International Conference on Environment and Electrical Engineering and 2017 IEEE Industrial and Commercial Power Systems Europe (EEEIC/I&CPS Europe), IEEE, 2017, pp. 1–6.

[22] L. Yuan, K. Meng, J. Huang, Z.Y. Dong, W. Zhang, X. Xie, Development of hvrt and lvrt control strategy for pmsg-based wind turbine generators, Energies 13 (20) (2020) 5442, https://doi.org/10.3390/en13205442.

[23] X. Zeng, T. Liu, S. Wang, Y. Dong, Z. Chen, Comprehensive coordinated control strategy of pmsg-based wind turbine for providing frequency regulation services, IEEE Access 7 (2019) 63944–63953, https://doi.org/10.1109/ACCESS.2019.2915308.

[24] H. Matayoshi, A.M. Howlader, M. Datta, T. Senjyu, Control strategy of pmsg based wind energy conversion system under strong wind conditions, Energy Sustain. Dev. 45 (2018) 211–218, https://doi.org/10.1016/j.esd.2018.07.001.

[25] J. Pande, P. Nasikkar, K. Kotecha, V. Varadarajan, A review of maximum power point tracking algorithms for wind energy conversion systems, J. Marine Sci. Eng. 9 (11) (2021) 1187, https://doi.org/10.3390/jmse9111187.

[26] M.A. Abdullah, A. Yatim, C.W. Tan, R. Saidur, A review of maximum power point tracking algorithms for wind energy systems, Renew. Sustain. Energy Rev. 16 (5) (2012) 3220–3227, https://doi.org/10.1016/j.rser.2012.02.016.

[27] H.H. Mousa, A.-R. Youssef, E.E. Mohamed, State of the art perturb and observe mppt algorithms based wind energy conversion systems: a technology review, Int. J. Electr. Power Energy Syst. 126 (2021) 106598, https://doi.org/10.1016/j.ijepes.2020.106598.

[28] M.Z. Malik, M.H. Baloch, M. Gul, G.S. Kaloi, S.T. Chauhdary, A.A. Memon, A research on conventional and modern algorithms for maximum power extraction from wind energy conversion system: a review, Environ. Sci. Pollut. Res. 28 (5) (2021) 5020–5035, https://doi.org/10.1007/s11356-020-11558-6.

[29] E. Shehata, A comparative study of current control schemes for a direct-driven pmsg wind energy generation system, Electr. Power Syst. Res. 143 (2017) 197–205, https://doi.org/10.1016/j.epsr.2016.10.039.

[30] E.J.N. Menezes, A.M. Araújo, N.S.B. Da Silva, A review on wind turbine control and its associated methods, J. Clean. Prod. 174 (2018) 945–953, https://doi.org/10.1016/j.jclepro.2017.10.297.

[31] R. Tiwari, N.R. Babu, Recent developments of control strategies for wind energy conversion system, Renew. Sustain. Energy Rev. 66 (2016) 268–285, https://doi.org/10.1016/j.rser.2016.08.005.

[32] B. Majout, H. El Alami, H. Salime, N. Zine Laabidine, Y. El Mourabit, S. Motahhir, M. Bouderbala, M. Karim, B. Bossoufi, A review on popular control applications in wind energy conversion system based on permanent magnet generator pmsg, Energies 15 (17) (2022) 6238, https://doi.org/10.3390/en15176238.

[33] V. Yaramasu, A. Dekka, M.J. Durán, S. Kouro, B. Wu, Pmsg-based wind energy conversion systems: survey on power converters and controls, IET Electr. Power Appl. 11 (6) (2017) 956–968, https://doi.org/10.1049/iet-epa.2016.0799.

[34] J.G. Njiri, D. Söffker, State-of-the-art in wind turbine control: trends and challenges, Renew. Sustain. Energy Rev. 60 (2016) 377–393, https://doi.org/10.1016/j.rser.2016.01.110.

[35] S.A. Papathanassiou, M.P. Papadopoulos, Mechanical stresses in fixed-speed wind turbines due to network disturbances, IEEE Trans. Energy Convers. 16 (4) (2001) 361–367, https://doi.org/10.1109/60.969476.

[36] J. Dai, X. Yang, L. Wen, Development of wind power industry in China: a comprehensive assessment, Renew. Sustain. Energy Rev. 97 (2018) 156–164, https://doi.org/10.1016/j.rser.2018.08.044.

[37] F. You, S. Shaik, M. Rokonuzzaman, K.S. Rahman, W.-S. Tan, Fire risk assessments and fire protection measures for wind turbines: a review, Heliyon (2023), https://doi.org/10.1016/j.heliyon.2023.e19664.

[38] H. Polinder, J.A. Ferreira, B.B. Jensen, A.B. Abrahamsen, K. Atallah, R.A. McMahon, Trends in wind turbine generator systems, IEEE J. Emerg. Sel. Top. Power Electron. 1 (3) (2013) 174–185, https://doi.org/10.1109/JESTPE.2013.2280428.

[39] G. Mayilsamy, S.R. Lee, Y.H. Joo, An improved model predictive control of back-to-back three-level npc converters with virtual space vectors for high power pmsg-based wind energy conversion systems, ISA Trans. 143 (2023) 503–524, https://doi.org/10.1016/j.isatra.2023.09.033.

[40] Y. Li, Z. Xu, K.P. Wong, Advanced control strategies of pmsg-based wind turbines for system inertia support, IEEE Trans. Power Syst. 32 (4) (2016) 3027–3037, https://doi.org/10.1109/TPWRS.2016.2616171.

[41] N. Elaadouli, R. Lajouad, A. El Magri, A. Watil, A. Mansouri, I. El Myasse, An improved control for a stand-alone wec system involving a Vienna rectifier with battery energy storage management, J. Energy Storage 76 (2024) 109716, https://doi.org/10.1016/j.est.2023.109716.

[42] A. Watil, A. El Magri, R. Lajouad, A. Raihani, F. Giri, Multi-mode control strategy for a stand-alone wind energy conversion system with battery energy storage, J. Energy Storage 51 (2022) 104481, https://doi.org/10.1016/j.est.2022.104481.

[43] A. Mansouri, A. El Magri, R. Lajouad, F. Giri, M. said Adouairi, B. Bossoufi, Nonlinear observer with reduced sensors for wecs involving Vienna rectifiers—theoretical design and experimental evaluation, Electr. Power Syst. Res. 225 (2023) 109847, https://doi.org/10.1016/j.epsr.2023.109847.

[44] S. Datta, S. Deb, A. Datta, S. Adhikari, B. Roy, Grid connected pmsg based wind energy conversion system using back-to-back converter, in: International Conference on Innovation in Modern Science and Technology, Springer, 2019, pp. 373–382.

[45] M.A. Abdullah, T. Al-Hadhrami, C.W. Tan, A.H. Yatim, Towards green energy for smart cities: particle swarm optimization based mppt approach, IEEE Access 6 (2018) 58427–58438, https://doi.org/10.1109/ACCESS.2018.2874525.

[46] G. Zhuo, J.D. Hostettler, P. Gu, X. Wang, Robust sliding mode control of permanent magnet synchronous generator-based wind energy conversion systems, Sustainability 8 (12) (2016) 1265, https://doi.org/10.3390/su8121265.

[47] Y. Xia, K.H. Ahmed, B.W. Williams, Wind turbine power coefficient analysis of a new maximum power point tracking technique, IEEE Trans. Ind. Electron. 60 (3) (2012) 1122–1132, https://doi.org/10.1109/TIE.2012.2206332.

[48] K. Mehran, N. Rezaei, C. Cossar, A model-based implementation of an mppt technique and a control system for a variable speed wind turbine pmsg, Int. J. Model. Identif. Control (2018), https://doi.org/10.1504/IJMIC.2019.096833.

[49] T.N. Gupta, S. Murshid, B. Singh, Power quality improvement of single phase weak grid interfaced hybrid solar pv and wind system using double fundamental signal extracter-based control, IET Gener. Transm. Distrib. 13 (17) (2019) 3988–3998, https://doi.org/10.1049/iet-gtd.2018.6647.

[50] H. Shutari, N. Saad, N.B.M. Nor, M.F.N. Tajuddin, M. Magzoub, Control strategies of power electronic converter for grid-tied variable low-speed wind turbine, in: AIP Conference Proceedings, vol. 2564, AIP Publishing, 2023.

[51] S.D. Ahmed, F.S. Al-Ismail, M. Shafiullah, F.A. Al-Sulaiman, I.M. El-Amin, Grid integration challenges of wind energy: a review, IEEE Access 8 (2020) 10857–10878, https://doi.org/10.1109/ACCESS.2020.2964896.

[52] Y. Zhu, S. Liu, W. Wang, Comprehensive coordinated control strategy of pmsg-based wind turbine for system inertia support, IET Renew. Power Gener. 15 (9) (2021) 1915–1926, https://doi.org/10.1049/rpg2.12115.

[53] H. Shutari, C.L. Wooi, H.A. Hamid, M.I. Mousa, W.S. Tan, H. Nabipour-Afrouzi, Modelling and simulation of definite time over current relay for radial systems protection, J. Adv. Res. Dyn. Control Syst. 11 (12-Special Issue) (2019) 785–794, https://doi.org/10.5373/JARDCS/V11SP12/20193277.

[54] F. Blaabjerg, M. Liserre, K. Ma, Power electronics converters for wind turbine systems, IEEE Trans. Ind. Appl. 48 (2) (2011) 708–719, https://doi.org/10.1109/TIA.2011.2181290.

[55] L. Aleksandr, G. Demidova, O. Alassaf, D. Lukichev, A. Rassõlkin, T. Vaimann, Mppt algorithms for wind turbines: review and comparison, in: 2022 29th International Workshop on Electric Drives: Advances in Power Electronics for Electric Drives (IWED), IEEE, 2022, pp. 1–6.

[56] A. Gambier, Modelling the wind turbine by using the tip-speed ratio for estimation and control, Energies 15 (24) (2022) 9454, https://doi.org/10.3390/en15249454.

[57] A. Bakbak, H.T. Canseven, M. Ayaz, M. Altıntaş, E. Meşe, Maximizing energy extraction from direct grid coupled pmsg for wind energy conversion systems, IEEE Trans. Ind. Appl. 58 (3) (2022) 3888–3900, https://doi.org/10.1109/TIA.2022.3160141.

[58] J. Chen, W. Yao, C.-K. Zhang, Y. Ren, L. Jiang, Design of robust mppt controller for grid-connected pmsg-based wind turbine via perturbation observation based nonlinear adaptive control, Renew. Energy 134 (2019) 478–495, https://doi.org/10.1016/j.renene.2018.11.048.

[59] D. Pathak, S. Bhati, P. Gaur, Fractional-order nonlinear pid controller based maximum power extraction method for a direct-driven wind energy system, Int. Trans. Electr. Energy Syst. 30 (12) (2020) e12641, https://doi.org/10.1002/2050-7038.12641.

[60] Y. Joo, et al., Integral sliding mode control for increasing maximum power extraction efficiency of variable-speed wind energy system, Int. J. Electr. Power Energy Syst. 139 (2022) 107958, https://doi.org/10.1016/j.ijepes.2022.107958.

[61] C.M. Parker, M.C. Leftwich, The effect of tip speed ratio on a vertical axis wind turbine at high Reynolds numbers, Exp. Fluids 57 (5) (2016) 1–11, https://doi.org/10.1007/s00348-016-2155-3.

[62] H.H. Mousa, A.-R. Youssef, E.E. Mohamed, Variable step size p&o mppt algorithm for optimal power extraction of multi-phase pmsg based wind generation system, Int. J. Electr. Power Energy Syst. 108 (2019) 218–231, https://doi.org/10.1016/j.ijepes.2018.12.044.

[63] D. Song, J. Yang, Z. Cai, M. Dong, M. Su, Y. Wang, Wind estimation with a non-standard extended Kalman filter and its application on maximum power extraction for variable speed wind turbines, Appl. Energy 190 (2017) 670–685, https://doi.org/10.1016/j.apenergy.2016.12.132.

[64] J.G. González-Hernández, R. Salas-Cabrera, R. Vázquez-Bautista, L.M. Ong-de-la Cruz, J. Rodríguez-Guillén, A novel mppt pi discrete reverse-acting controller for a wind energy conversion system, Renew. Energy 178 (2021) 904–915, https://doi.org/10.1016/j.renene.2021.06.106.

[65] S. Lawan, W. Abidin, T. Masri, Implementation of a topographic artificial neural network wind speed prediction model for assessing onshore wind power potential in Sibu, Sarawak, Egypt. J. Remote Sens. Space Sci. 23 (1) (2020) 21–34, https://doi.org/10.1016/j.ejrs.2019.08.003.

[66] K. Palanimuthu, G. Mayilsamy, S.R. Lee, S.Y. Jung, Y.H. Joo, Fault ride-through for pmvg-based wind turbine system using coordinated active and reactive power control strategy, IEEE Trans. Ind. Electron. (2022), https://doi.org/10.1109/TIE.2022.3194638.

[67] R.I. Putri, M. Pujiantara, A. Priyadi, T. Ise, M.H. Purnomo, Maximum power extraction improvement using sensorless controller based on adaptive perturb and observe algorithm for pmsg wind turbine application, IET Electr. Power Appl. 12 (4) (2018) 455–462, https://doi.org/10.1049/iet-epa.2017.0603.

[68] A.A. Yesudhas, Y.H. Joo, S.R. Lee, Reference model adaptive control scheme on pmvg-based wecs for mppt under a real wind speed, Energies 15 (9) (2022) 3091, https://doi.org/10.3390/en15093091.

[69] D. Jena, S. Rajendran, A review of estimation of effective wind speed based control of wind turbines, Renew. Sustain. Energy Rev. 43 (2015) 1046–1062, https://doi.org/10.1016/j.rser.2014.11.088.

[70] F. Jaramillo-Lopez, G. Kenne, F. Lamnabhi-Lagarrigue, A novel online training neural network-based algorithm for wind speed estimation and adaptive control of pmsg wind turbine system for maximum power extraction, Renew. Energy 86 (2016) 38–48, https://doi.org/10.1016/j.renene.2015.07.071.

[71] D. Song, J. Yang, X. Fan, Y. Liu, A. Liu, G. Chen, Y.H. Joo, Maximum power extraction for wind turbines through a novel yaw control solution using predicted wind directions, Energy Convers. Manag. 157 (2018) 587–599, https://doi.org/10.1016/j.enconman.2017.12.019.

[72] H. Al-Ghossini, F. Locment, M. Sechilariu, L. Gagneur, C. Forgez, Adaptive-tuning of extended Kalman filter used for small scale wind generator control, Renew. Energy 85 (2016) 1237–1245, https://doi.org/10.1016/j.renene.2015.07.073.

[73] Y. Daili, J.-P. Gaubert, Implementation of a new maximum power point tracking control strategy for small wind energy conversion systems without mechanical sensors, Energy Convers. Manag. 97 (2015) 298–306, https://doi.org/10.1016/j.enconman.2015.03.062.

[74] A.J. Balbino, B.d.S. Nora, T.B. Lazzarin, An improved mechanical sensorless maximum power point tracking method for permanent-magnet synchronous generator-based small wind turbines systems, IEEE Trans. Ind. Electron. 69 (5) (2021) 4765–4775, https://doi.org/10.1109/TIE.2021.3084176.

[75] M. Yin, W. Li, C.Y. Chung, L. Zhou, Z. Chen, Y. Zou, Optimal torque control based on effective tracking range for maximum power point tracking of wind turbines under varying wind conditions, IET Renew. Power Gener. 11 (4) (2017) 501–510, https://doi.org/10.1049/iet-rpg.2016.0635.

[76] Y. El Mourabit, A. Derouich, A. El Ghzizal, N. El Ouanjli, O. Zamzoum, Nonlinear backstepping control for pmsg wind turbine used on the real wind profile of the Dakhla-Morocco city, Int. Trans. Electr. Energy Syst. 30 (4) (2020) e12297, https://doi.org/10.1002/2050-7038.12297.

[77] M.M. Mahmoud, B.S. Atia, M.K. Ratib, M.M. Aly, A.E. Elwakeel, A.-M.M. Abdel-Rahim, Investigations on otc-mppt strategy and frt capability for pmsg wind system with the support of optimized wind side controller based on gwo technique, Energy 4 (4) (2021), https://doi.org/10.38028/esr.2021.04.0007.

[78] M.M. Mahmoud, M.M. Aly, H.S. Salama, A.-M.M. Abdel-Rahim, A combination of an otc based mppt and fuzzy logic current control for a wind-driven pmsg under variability of wind speed, Energy Syst. 13 (4) (2022) 1075–1098, https://doi.org/10.1007/s12667-021-00468-2.

[79] K. Palanimuthu, G. Mayilsamy, S.R. Lee, S.Y. Jung, Y.H. Joo, Comparative analysis of maximum power extraction and control methods between pmsg and pmvg-based wind turbine systems, Int. J. Electr. Power Energy Syst. 143 (2022) 108475, https://doi.org/10.1016/j.ijepes.2022.108475.

[80] X. Zhang, Y. Zhang, S. Hao, L. Wu, W. Wei, An improved maximum power point tracking method based on decreasing torque gain for large scale wind turbines at low wind sites, Electr. Power Syst. Res. 176 (2019) 105942, https://doi.org/10.1016/j.epsr.2019.105942.

[81] X. Zhang, C. Huang, S. Hao, F. Chen, J. Zhai, An improved adaptive-torque-gain mppt control for direct-driven pmsg wind turbines considering wind farm turbulences, Energies 9 (11) (2016) 977, https://doi.org/10.3390/en9110977.

[82] J. Chen, W. Yao, Q. Lu, Y. Ren, W. Duan, J. Kan, L. Jiang, Adaptive active fault-tolerant mppt control of variable-speed wind turbine considering generator actuator failure, Int. J. Electr. Power Energy Syst. 143 (2022) 108443, https://doi.org/10.1016/j.ijepes.2022.108443.

[83] J. Chen, K. Cai, T. Lin, Adaptive maximum power point tracking control strategy for variable-speed wind energy conversion systems with constant tracking speed, in: 2019 22nd International Conference on Electrical Machines and Systems (ICEMS), IEEE, 2019, pp. 1–5.

[84] L. Li, Y. Ren, J. Chen, K. Shi, L. Jiang, Modified p&o approach based detection of the optimal power-speed curve for mppt of wind turbines, in: Energy Internet, Springer, 2020, pp. 137–155.

[85] B.K. Ramasamy, A. Palaniappan, S. Mohamed Yakoh, Direct-drive low-speed wind energy conversion system incorporating axial-type permanent magnet generator and z-source inverter with sensorless maximum power point tracking controller, IET Renew. Power Gener. 7 (3) (2013) 284–295, https://doi.org/10.1049/iet-rpg.2012.0248.

[86] S. Morimoto, H. Nakayama, M. Sanada, Y. Takeda, Sensorless output maximization control for variable-speed wind generation system using ipmsg, IEEE Trans. Ind. Appl. 41 (1) (2005) 60–67, https://doi.org/10.1109/TIA.2004.841159.

[87] J. Xi, H. Geng, S. Ma, Y. Chi, G. Yang, Inertial response characteristics analysis and optimisation of pmsg-based vsg-controlled wecs, IET Renew. Power Gener. 12 (15) (2018) 1741–1747, https://doi.org/10.1049/iet-rpg.2018.5250.

[88] Y. Zhu, Z. Wang, X. Guo, Z. Wei, An improved kinetic energy control strategy for power smoothing of pmsg-wecs based on low pass filter and fuzzy logic controller, Electr. Power Syst. Res. 214 (2023) 108816, https://doi.org/10.1016/j.epsr.2022.108816.

[89] L.M. Shankareppagol, S.N. Hampannavar, S.N. Doadamani, Performance analysis of p&o and inc mppt for wecs, in: 2018 3rd International Conference for Convergence in Technology (I2CT), IEEE, 2018, pp. 1–8.

[90] A.F. Tazay, A.M.A. Ibrahim, O. Noureldeen, I. Hamdan, Modeling, control, and performance evaluation of grid-tied hybrid pv/wind power generation system: case study of Gabel El-Zeit region, Egypt, IEEE Access 8 (2020) 96528–96542, https://doi.org/10.1109/ACCESS.2020.2993919.

[91] D. Zammit, C.S. Staines, A. Micallef, M. Apap, J. Licari, Incremental current based mppt for a pmsg micro wind turbine in a grid-connected dc microgrid, Energy Proc. 142 (2017) 2284–2294, https://doi.org/10.1016/j.egypro.2017.12.631.

[92] K.N. Yu, C.K. Liao, Applying novel fractional order incremental conductance algorithm to design and study the maximum power tracking of small wind power systems, J. Appl. Res. Technol. 13 (2) (2015) 238–244, https://doi.org/10.1016/j.jart.2015.06.002.

[93] B. Tidhaf, et al., A new maximum power point tracking based on neural networks and incremental conductance for wind energy conversion system, in: E3S Web of Conferences, vol. 336, EDP Sciences, 2022, p. 00055.

[94] G. Pathak, B. Singh, B. Panigrahi, Isolated microgrid employing pmbldcg for wind power generation and synchronous reluctance generator for dg system, in: 2014 IEEE 6th India International Conference on Power Electronics (IICPE), IEEE, 2014, pp. 1–6.

[95] M. Abdelateef Mostafa, E.A. El-Hay, M.M. ELkholy, Recent trends in wind energy conversion system with grid integration based on soft computing methods: comprehensive review, comparisons and insights, Arch. Comput. Methods Eng. (2022) 1–40, https://doi.org/10.1007/s11831-022-09842-4.

[96] D. Kumar, K. Chatterjee, A review of conventional and advanced mppt algorithms for wind energy systems, Renew. Sustain. Energy Rev. 55 (2016) 957–970, https://doi.org/10.1016/j.rser.2015.11.013.

[97] E.H. Dursun, H. Koyuncu, A.A. Kulaksiz, A novel unified maximum power extraction framework for pmsg based wecs using chaotic particle swarm optimization derivatives, Int. J. Eng. Sci. Technol. 24 (1) (2021) 158–170, https://doi.org/10.1016/j.jestch.2020.05.005.

[98] M.A. Abdullah, A.Q. Al-Shetwi, M. Mansor, M. Hannan, C.W. Tan, A. Yatim, Linear quadratic regulator controllers for regulation of the dc-bus voltage in a hybrid energy system: modeling, design and experimental validation, Sustain. Energy Technol. Assessments 50 (2022) 101880, https://doi.org/10.1016/j.seta.2021.101880.

[99] A. Urtasun, P. Sanchis, I. San Martin, J. López, L. Marroyo, Modeling of small wind turbines based on pmsg with diode bridge for sensorless maximum power tracking, Renew. Energy 55 (2013) 138–149, https://doi.org/10.1016/j.renene.2012.12.035.

[100] Q.-V. Ngo, T.-T. Nguyen, The mppt algorithm combined with pitch angle control for the small-scale wind turbine in a wide speed range, Int. J. Power Electron. Drive Syst. 12 (3) (2021) 1482, https://doi.org/10.11591/ijpeds.v12.i3.pp1482-1493.

[101] H.-B. Zhang, J. Fletcher, N. Greeves, S. Finney, B. Williams, One-power-point operation for variable speed wind/tidal stream turbines with synchronous generators, IET Renew. Power Gener. 5 (1) (2011) 99–108, https://doi.org/10.1049/iet-rpg.2009.0207.

[102] C. Wei, Z. Zhang, W. Qiao, L. Qu, An adaptive network-based reinforcement learning method for mppt control of pmsg wind energy conversion systems, IEEE Trans. Power Electron. 31 (11) (2016) 7837–7848, https://doi.org/10.1109/TPEL.2016.2514370.

[103] C.-T. Pan, Y.-L. Juan, A novel sensorless mppt controller for a high-efficiency microscale wind power generation system, IEEE Trans. Energy Convers. 25 (1) (2009) 207–216, https://doi.org/10.1109/TEC.2009.2032604.

[104] B. Desalegn, D. Gebeyehu, B. Tamrat, Wind energy conversion technologies and engineering approaches to enhancing wind power generation: a review, Heliyon 8 (11) (2022), https://doi.org/10.1016/j.heliyon.2022.e11263.

[105] J. Aourir, F. Locment, Limited power point tracking for a small-scale wind turbine intended to be integrated in a dc microgrid, Appl. Sci. 10 (22) (2020) 8030, https://doi.org/10.3390/app10228030.

[106] B. Singh, F. Chishti, S. Murshid, Disturbance rejection through adaptive frequency estimation observer for wind-solar integrated ac microgrid, IEEE Trans. Ind. Inform. 15 (11) (2019) 6035–6047, https://doi.org/10.1109/TII.2019.2923375.

[107] A.-R. Youssef, A.I. Ali, M.S. Saeed, E.E. Mohamed, Advanced multi-sector p&o maximum power point tracking technique for wind energy conversion system, Int. J. Electr. Power Energy Syst. 107 (2019) 89–97, https://doi.org/10.1016/j.ijepes.2018.10.034.

[108] B. Meghni, M. Ouada, S. Saad, A novel improved variable-step-size p&o mppt method and effective supervisory controller to extend optimal energy management in hybrid wind turbine, Electr. Eng. 102 (2) (2020) 763–778, https://doi.org/10.1007/s00202-019-00911-9.

[109] R. Syahputra, I. Soesanti, Performance improvement for small-scale wind turbine system based on maximum power point tracking control, Energies 12 (20) (2019) 3938, https://doi.org/10.3390/en12203938.

[110] H.H. Mousa, A.-R. Youssef, E.E. Mohamed, Study of robust adaptive step-sizes p&o mppt algorithm for high-inertia wt with direct-driven multiphase pmsg, Int. Trans. Electr. Energy Syst. 29 (10) (2019) e12090, https://doi.org/10.1002/2050-7038.12090.

[111] H.H. Mousa, A.-R. Youssef, E.E. Mohamed, Modified p&o mppt algorithm for optimal power extraction of five-phase pmsg based wind generation system, SN Appl. Sci. 1 (8) (2019) 1–16, https://doi.org/10.1007/s42452-019-0878-5.

[112] H. Gouabi, A. Hazzab, M. Rezkallah, M. Habbab, H. Ibrahim, A. Chandra, Fuzzy logic size and frequency scheduling of dp-p&o perturbation for wecs mppt control, in: 2023 IEEE Industry Applications Society Annual Meeting (IAS), IEEE, 2023, pp. 1–6.

[113] M. Karabacak, A new perturb and observe based higher order sliding mode mppt control of wind turbines eliminating the rotor inertial effect, Renew. Energy 133 (2019) 807–827, https://doi.org/10.1016/j.renene.2018.10.079.

[114] A. Merabet, M.A. Islam, R. Beguenane, A. Trznadlowski, Multivariable control algorithm for laboratory experiments in wind energy conversion, Renew. Energy 83 (2015) 162–170, https://doi.org/10.1016/j.renene.2015.04.031.

[115] C. Ramos-Paja, A. Saavedra-Montes, E. Arango, Maximum power point tracking in wind farms by means of a multivariable algorithm, in: 2012 Workshop on Engineering Applications, IEEE, 2012, pp. 1–6.

[116] N.E. Zakzouk, Continuous input current buck dc/dc converter for small-size wind energy systems featuring current sensorless mppt control, Sci. Rep. 14 (1) (2024) 380, https://doi.org/10.1038/s41598-023-50442-2.

[117] M.M. Ali, A.-r. Youssef, A.S. Ali, G. Abdel-Jaber, Variable step size po mppt algorithm using model reference adaptive control for optimal power extraction, Int. Trans. Electr. Energy Syst. 30 (1) (2020) e12151, https://doi.org/10.1002/2050-7038.12151.

[118] A.-R. Youssef, H.H. Mousa, E.E. Mohamed, Development of self-adaptive p&o mppt algorithm for wind generation systems with concentrated search area, Renew. Energy 154 (2020) 875–893, https://doi.org/10.1016/j.renene.2020.03.050.

[119] H.H. Mousa, A.-R. Youssef, E.E. Mohamed, Hybrid and adaptive sectors p&o mppt algorithm based wind generation system, Renew. Energy 145 (2020) 1412–1429, https://doi.org/10.1016/j.renene.2019.06.078.

[120] Y. Daili, J.-P. Gaubert, L. Rahmani, New control strategy for fast-efficient maximum power point tracking without mechanical sensors applied to small wind energy conversion system, J. Renew. Sustain. Energy 7 (4) (2015) 043102, https://doi.org/10.1063/1.4923394.

[121] R.M. Linus, P. Damodharan, Maximum power point tracking method using a modified perturb and observe algorithm for grid connected wind energy conversion systems, IET Renew. Power Gener. 9 (6) (2015) 682–689, https://doi.org/10.1049/iet-rpg.2014.0070.

[122] S.M.R. Kazmi, H. Goto, H.-J. Guo, O. Ichinokura, A novel algorithm for fast and efficient speed-sensorless maximum power point tracking in wind energy conversion systems, IEEE Trans. Ind. Electron. 58 (1) (2010) 29–36, https://doi.org/10.1109/TIE.2010.2044732.

[123] B. Mendi, M. Pattnaik, G. Srungavarapu, A single current sensor based adaptive step size mppt control of a small scale variable speed wind energy conversion system, Appl. Energy 357 (2024) 122492, https://doi.org/10.1016/j.apenergy.2023.122492.

[124] Hemanth Kumar, B. Mekalathur, Balasubramanian Saravanan, Padmanaban Sanjeevikumar, Frede Blaabjerg, Review on control techniques and methodologies for maximum power extraction from wind energy systems, IET Renew. Power Gener. 12 (14) (2018) 1609–1622, https://doi.org/10.1049/iet-rpg.2018.5206.

[125] H.H. Mousa, A.-R. Youssef, E.E. Mohamed, Adaptive p&o mppt algorithm based wind generation system using realistic wind fluctuations, Int. J. Electr. Power Energy Syst. 112 (2019) 294–308, https://doi.org/10.1016/j.ijepes.2019.04.038.

[126] M.H. HH, A.-R. Youssef, M.E. EM, Improved perturb and observe mppt algorithm of multi-phase pmsg based wind energy conversion system, in: 2019 21st International Middle East Power Systems Conference (MEPCON), IEEE, 2019, pp. 97–102.

[127] A.R. Nateghi, H.K. Karegar, S. Bagheri, Maximum power point tracking of permanent magnet wind turbines equipped with direct matrix converter, J. Renew. Sustain. Energy 6 (5) (2014) 053123, https://doi.org/10.1063/1.4898365.

[128] V. Nayanar, N. Kumaresan, N.A. Gounden, A single-sensor-based mppt controller for wind-driven induction generators supplying dc microgrid, IEEE Trans. Power Electron. 31 (2) (2015) 1161–1172, https://doi.org/10.1109/TPEL.2015.2420568.

[129] V. Agarwal, R.K. Aggarwal, P. Patidar, C. Patki, A novel scheme for rapid tracking of maximum power point in wind energy generation systems, IEEE Trans. Energy Convers. 25 (1) (2009) 228–236, https://doi.org/10.1109/TEC.2009.2032613.

[130] Z.A. Alrowaili, M.M. Ali, A. Youssef, H.H. Mousa, A.S. Ali, G.T. Abdel-Jaber, M. Ezzeldien, F. Gami, Robust adaptive hcs mppt algorithm-based wind generation system using model reference adaptive control, Sensors 21 (15) (2021) 5187, https://doi.org/10.3390/s21155187.

[131] H. Shutari, T. Ibrahim, N.B.M. Nor, N. Saad, M.F.N. Tajuddin, H.Q. Abdulrab, Development of a novel efficient maximum power extraction technique for grid-tied vswt system, IEEE Access 10 (2022) 101922–101935, https://doi.org/10.1109/ACCESS.2022.3208583.

[132] J.C. Hui, A. Bakhshai, P.K. Jain, An energy management scheme with power limit capability and an adaptive maximum power point tracking for small standalone pmsg wind energy systems, IEEE Trans. Power Electron. 31 (7) (2015) 4861–4875, https://doi.org/10.1109/TPEL.2015.2478402.

[133] H. Kala, K. Sandhu, Selection of wind turbine for mppt, in: 2016 International Conference on Microelectronics, Computing and Communications (MicroCom), IEEE, 2016, pp. 1–4.

[134] A.S. Nambiar, G.M. Raja, K. Harindran, P. Rajan, S.S. Sankar, V.J. Sankar, Design and development of a maximum power point tracker and its testing setup for wind energy conversion system with laboratory level devices, in: 2017 International Conference on Technological Advancements in Power and Energy (TAP Energy), IEEE, 2017, pp. 1–5.

[135] K. Chaicharoenaudomrung, K. Areerak, K. Areerak, S. Bozhko, C.I. Hill, Maximum power point tracking for stand-alone wind energy conversion system using flc-p&o method, IEEJ Trans. Electr. Electron. Eng. 15 (12) (2020) 1723–1733, https://doi.org/10.1002/tee.23246.

[136] V. Govinda Chowdary, V. Udhay Sankar, D. Mathew, C. Hussaian Basha, C. Rani, Hybrid fuzzy logic-based mppt for wind energy conversion system, in: Soft Computing for Problem Solving, Springer, 2020, pp. 951–968.

[137] M.J. Khan, L. Mathew, Fuzzy logic controller-based mppt for hybrid photo-voltaic/wind/fuel cell power system, Neural Comput. Appl. 31 (10) (2019) 6331–6344, https://doi.org/10.1007/s00521-018-3456-7.

[138] M.K. Asy'Ari, M.B. Toriki, B.E. Apriajumita, et al., Design of fuzzy logic control based on sepic converter for mppt on wind turbine, in: 2022 International Seminar on Intelligent Technology and Its Applications (ISITIA), IEEE, 2022, pp. 444–448.

[139] R. Tiwari, N.R. Babu, Fuzzy logic based mppt for permanent magnet synchronous generator in wind energy conversion system, IFAC-PapersOnLine 49 (1) (2016) 462–467, https://doi.org/10.1016/j.ifacol.2016.03.097.

[140] A. El Yaakoubi, A. Asselman, A. Djebli, et al., A mppt strategy based on fuzzy control for a wind energy conversion system, Proc. Technol. 22 (2016) 697–704, https://doi.org/10.1016/j.protcy.2016.01.145.

[141] A.P. Marugán, F.P.G. Márquez, J.M.P. Perez, D. Ruiz-Hernández, A survey of artificial neural network in wind energy systems, Appl. Energy 228 (2018) 1822–1836, https://doi.org/10.1016/j.apenergy.2018.07.084.

[142] S. Aher, P. Chavan, R. Deshmukh, V. Pawar, M. Thakre, Designing and software realization of an ann-based mppt-fed bladeless wind power generation, Glob. Transitions Proc. 2 (2) (2021) 584–588, https://doi.org/10.1016/j.gltp.2021.08.054.

[143] S. Tripathi, A. Tiwari, D. Singh, Grid-integrated permanent magnet synchronous generator based wind energy conversion systems: a technology review, Renew. Sustain. Energy Rev. 51 (2015) 1288–1305, https://doi.org/10.1016/j.rser.2015.06.060.

[144] M.A.M. Khan, M.K. Hossain, Neural network-based control for wind turbine system with pmsg: a case study for Hafar Al-Batin, Arab. J. Sci. Eng. 47 (11) (2022) 14969–14981, https://doi.org/10.1007/s13369-022-07003-0.

[145] R. Tiwari, K. Krishnamurthy, R.B. Neelakandan, S. Padmanaban, P.W. Wheeler, Neural network based maximum power point tracking control with quadratic boost converter for pmsg—wind energy conversion system, Electronics 7 (2) (2018) 20, https://doi.org/10.3390/electronics7020020.

[146] K. Kumar, N.R. Babu, K. Prabhu, Design and analysis of rbfn-based single mppt controller for hybrid solar and wind energy system, IEEE Access 5 (2017) 15308–15317, https://doi.org/10.1109/ACCESS.2017.2733555.

[147] R. Sitharthan, M. Karthikeyan, D.S. Sundar, S. Rajasekaran, Adaptive hybrid intelligent mppt controller to approximate effectual wind speed and optimal rotor speed of variable speed wind turbine, ISA Trans. 96 (2020) 479–489, https://doi.org/10.1016/j.isatra.2019.05.029.

[148] M. Yuhendri, M. Muskhir, T. Taali, A novel optimum tip speed ratio control of low speed wind turbine generator based on type-2 fuzzy system, Bull. Electr. Eng. Informatics 8 (4) (2019) 1189–1197, https://doi.org/10.11591/eei.v8i4.1450.

[149] P. Rajesh, F.H. Shajin, K. Cherukupalli, An efficient hybrid tunicate swarm algorithm and radial basis function searching technique for maximum power point tracking in wind energy conversion system, J. Eng. Des. Technol. (2021), https://doi.org/10.1108/JEDT-12-2020-0494.

[150] S. Belaid, D. Rekioua, A. Oubelaid, D. Ziane, T. Rekioua, A power management control and optimization of a wind turbine with battery storage system, J. Energy Storage 45 (2022) 103613, https://doi.org/10.1016/j.est.2021.103613.

[151] S. Lalouni, D. Rekioua, K. Idjdarene, A. Tounzi, Maximum power point tracking based hybrid hill-climb search method applied to wind energy conversion system, Electr. Power Compon. Syst. 43 (8–10) (2015) 1028–1038, https://doi.org/10.1080/15325008.2014.999143.

[152] J. Chen, T. Lin, C. Wen, Y. Song, Design of a unified power controller for variable-speed fixed-pitch wind energy conversion system, IEEE Trans. Ind. Electron. 63 (8) (2016) 4899–4908, https://doi.org/10.1109/TIE.2016.2547365.

[153] K. Dahmane, B. Bouachrine, M. Ajaamoum, B. Imodane, S. Mouslim, M. Benydir, et al., Hybrid mppt control: P&O and neural network for wind energy conversion system, J. Robotics Control 4 (1) (2023) 1–11, https://doi.org/10.18196/jrc.v4i1.16770.

[154] A.B. Asghar, X. Liu, Adaptive neuro-fuzzy algorithm to estimate effective wind speed and optimal rotor speed for variable-speed wind turbine, Neurocomputing 272 (2018) 495–504, https://doi.org/10.1016/j.neucom.2017.07.022.

[155] M. Badar, I. Ahmad, A.A. Mir, S. Ahmed, A. Waqas, An autonomous hybrid dc microgrid with ann-fuzzy and adaptive terminal sliding mode multi-level control structure, Control Eng. Pract. 121 (2022) 105036, https://doi.org/10.1016/j.conengprac.2021.105036.

[156] H. Gouabi, A. Hazzab, M. Habbab, M. Rezkallah, A. Chandra, Experimental implementation of a novel scheduling algorithm for adaptive and modified p&o mppt controller using fuzzy logic for wecs, Int. J. Adapt. Control Signal Process. 35 (9) (2021) 1732–1753, https://doi.org/10.1002/acs.3288.

[157] M.N. Uddin, N. Patel, Maximum power point tracking control of ipmsg incorporating loss minimization and speed sensorless schemes for wind energy system, IEEE Trans. Ind. Appl. 52 (2) (2015) 1902–1912, https://doi.org/10.1109/TIA.2015.2510507.

[158] B. Meghni, N. M'Sirdi, A. Saadoun, A novel maximum power tracking by vsas approach for permanent magnet direct drive wecs, Energy Proc. 83 (2015) 79–90, https://doi.org/10.1016/j.egypro.2015.12.198.

[159] J. Hussain, M.K. Mishra, Adaptive maximum power point tracking control algorithm for wind energy conversion systems, IEEE Trans. Energy Convers. 31 (2) (2016) 697–705, https://doi.org/10.1109/TEC.2016.2520460.

[160] H. Fathabadi, Maximum mechanical power extraction from wind turbines using novel proposed high accuracy single-sensor-based maximum power point tracking technique, Energy 113 (2016) 1219–1230, https://doi.org/10.1016/j.energy.2016.07.081.

[161] J.D. De Kooning, T.L. Vandoorn, J. Van de Vyver, B. Meersman, L. Vandevelde, Displacement of the maximum power point caused by losses in wind turbine systems, Renew. Energy 85 (2016) 273–280, https://doi.org/10.1016/j.renene.2015.06.052.

[162] İ. Yazici, E.K. Yaylaci, Maximum power point tracking for the permanent magnet synchronous generator-based wecs by using the discrete-time integral sliding mode controller with a chattering-free reaching law, IET Power Electron. 10 (13) (2017) 1751–1758, https://doi.org/10.1049/iet-pel.2017.0232.

[163] D. Song, J. Yang, M. Su, A. Liu, Y. Liu, Y.H. Joo, A comparison study between two mppt control methods for a large variable-speed wind turbine under different wind speed characteristics, Energies 10 (5) (2017) 613, https://doi.org/10.3390/en10050613.

[164] S. Heshmatian, D.A. Khaburi, M. Khosravi, A. Kazemi, A control scheme for maximizing the delivered power to the load in a standalonewind energy conversion system, Turk. J. Electr. Eng. Comput. Sci. 27 (4) (2019) 2998–3014, https://doi.org/10.3906/elk-1809-166.

[165] H. Ramadan, A.-R. Youssef, H.H. Mousa, E.E. Mohamed, An efficient variable-step p&o maximum power point tracking technique for grid-connected wind energy conversion system, SN Appl. Sci. 1 (12) (2019) 1–15, https://doi.org/10.1007/s42452-019-1716-5.

[166] H.H. Mousa, A.-R. Youssef, E.E. Mohamed, Optimal power extraction control schemes for five-phase pmsg based wind generation systems, Int. J. Eng. Sci. Technol. 23 (1) (2020) 144–155, https://doi.org/10.1016/j.jestch.2019.04.004.

[167] E.H. Dursun, A.A. Kulaksiz, Mppt control of pmsg based small-scale wind energy conversion system connected to dc-bus, Int. J. Emerg. Electr. Power Syst. 21 (2) (2020), https://doi.org/10.1515/ijeeps-2019-0188.

[168] M. Fannakh, M.L. Elhafyani, S. Zouggar, H. Zahboune, Performances mppt enhancement in pmsg wind turbine system using fuzzy logic control, in: International Conference on Electronic Engineering and Renewable Energy, Springer, 2020, pp. 797–807.

[169] D.R. Lopez-Flores, J.L. Duran-Gomez, M.I. Chacon-Murguia, A mechanical sensorless mppt algorithm for a wind energy conversion system based on a modular multilayer perceptron and a processor-in-the-loop approach, Electr. Power Syst. Res. 186 (2020) 106409, https://doi.org/10.1016/j.epsr.2020.106409.

[170] P.S. Babu, C. Sundarabalan, C. Balasundar, T.S. Krishnan, Fuzzy logic based optimal tip speed ratio mppt controller for grid connected wecs, Mater. Today Proc. 45 (2021) 2544–2550, https://doi.org/10.1016/j.matpr.2020.11.259.

[171] H.H. Mousa, A.-R. Youssef, I. Hamdan, M. Ahamed, E.E. Mohamed, Performance assessment of robust p&o algorithm using optimal hypothetical position of generator speed, IEEE Access 9 (2021) 30469–30485, https://doi.org/10.1109/ACCESS.2021.3059884.

[172] T. Syskakis, M. Ordonez, Mppt for small wind turbines: zero-oscillation sensorless strategy, in: 2019 IEEE 10th International Symposium on Power Electronics for Distributed Generation Systems (PEDG), IEEE, 2019, pp. 1060–1065.

[173] X. Jiao, X. Zhou, Q. Yang, Z. Zhang, W. Liu, J. Zhao, An improved optimal torque control based on estimated wind speed for wind turbines, in: 2022 13th Asian Control Conference (ASCC), IEEE, 2022, pp. 2024–2029.

[174] N. Sivakumar, A. Routray, N. Sajeev, F. Raju, G. Dhiman, Neural network based reinforcement learning for maximum power extraction of wind energy, in: 2022 IEEE 4th International Conference on Cybernetics, Cognition and Machine Learning Applications (ICCCMLA), IEEE, 2022, pp. 210–215.

[175] B. Belkacem, N. Bouhamri, L.A. Koridak, A. Allali, Fuzzy optimization strategy of the maximum power point tracking for a variable wind speed system, Int. J. Electr. Comput. Eng. 12 (4) (2022) 4264–4275, https://doi.org/10.11591/ijece.v12i4.pp4264-4275.

[176] R. Venkateswaran, B. Natesan, S.R. Lee, Y.H. Joo, Maximum power extraction for pmvg-based wecs using q-learning mppt algorithm with finite-time control scheme, IEEE Trans. Sustain. Energy 14 (1) (2022) 516–524, https://doi.org/10.1109/TSTE.2022.3218045.

[177] G. Zhang, Z. Li, B. Zhang, W.A. Halang, Power electronics converters: past, present and future, Renew. Sustain. Energy Rev. 81 (2018) 2028–2044, https://doi.org/10.1016/j.rser.2017.05.290.

[178] M. Hannan, M.H. Lipu, P.J. Ker, R. Begum, V.G. Agelidis, F. Blaabjerg, Power electronics contribution to renewable energy conversion addressing emission reduction: applications, issues, and recommendations, Appl. Energy 251 (2019) 113404, https://doi.org/10.1016/j.apenergy.2019.113404.

[179] M. Edrah, X. Zhao, W. Hung, P. Qi, B. Marshall, S. Baloch, A. Karcanias, Electromechanical interactions of full scale converter wind turbine with power oscillation damping and inertia control, Int. J. Electr. Power Energy Syst. 135 (2022) 107522, https://doi.org/10.1016/j.ijepes.2021.107522.

[180] M.H. Qais, H.M. Hasanien, S. Alghuwainem, Output power smoothing of wind power plants using self-tuned controlled smes units, Electr. Power Syst. Res. 178 (2020) 106056, https://doi.org/10.1016/j.epsr.2019.106056.

[181] D.P. Aguemon, R.G. Agbokpanzo, F. Dubas, A. Vianou, D. Chamagne, C. Espanet, Analysis on the topology and control of power electronics converters for wind energy conversion systems, Int. J. Res. Rev. 8 (8) (2021) 127–137, https://doi.org/10.52403/ijrr.20210819.

[182] Z. Ahmad, J.R. Torres, N. Veera Kumar, E. Rakhshani, P. Palensky, M. Van Der Meijden, A power hardware-in-the-loop based method for fapr compliance testing of the wind turbine converters control, Energies 13 (19) (2020) 5203, https://doi.org/10.3390/en13195203.

[183] O. Apata, D. Oyedokun, An overview of control techniques for wind turbine systems, Sci. Afr. 10 (2020) e00566, https://doi.org/10.1016/j.sciaf.2020.e00566.

[184] K.B. Tawfiq, A.S. Mansour, H.S. Ramadan, M. Becherif, E. El-Kholy, Wind energy conversion system topologies and converters: comparative review, Energy Proc. 162 (2019) 38–47, https://doi.org/10.1016/j.egypro.2019.04.005.

[185] T. Sadamoto, A. Chakrabortty, T. Ishizaki, J.-i. Imura, Dynamic modeling, stability, and control of power systems with distributed energy resources: handling faults using two control methods in tandem, IEEE Control Syst. Mag. 39 (2) (2019) 34–65, https://doi.org/10.1109/MCS.2018.2888680.

[186] A. Ahmedi, M. Barnes, V. Levi, J.C. Sanchez, C. Ng, P. McKeever, Modelling of wind turbine operation for enhanced power electronics reliability, IEEE Trans. Energy Convers. 37 (3) (2022) 1764–1776, https://doi.org/10.1109/TEC.2022.3144499.

[187] M. Aimene, A. Payman, B. Dakyo, Comparative study between flatness-based and field-oriented control methods of a grid-connected wind energy conversion system, Processes 10 (2) (2022) 378, https://doi.org/10.3390/pr10020378.

[188] Q. Guo, F. Xiao, C. Tu, F. Jiang, R. Zhu, J. Ye, J. Gao, An overview of series-connected power electronic converter with function extension strategies in the context of high-penetration of power electronics and renewables, Renew. Sustain. Energy Rev. 156 (2022) 111934, https://doi.org/10.1016/j.rser.2021.111934.

[189] S. Karyś, P. Stawczyk, Cost-effective power converters for small wind turbines, Energies 14 (18) (2021) 5906, https://doi.org/10.3390/en14185906.

[190] H.N.V. Pico, V. Gevorgian, Blackstart capability and survivability of wind turbines with fully rated converters, IEEE Trans. Energy Convers. 37 (4) (2022) 2482–2497, https://doi.org/10.1109/TEC.2022.3173903.

[191] B.P. Ganthia, S.K. Barik, B. Nayak, Wind turbines in energy conversion system: types & techniques, Renew. Energy Future Power Syst. (2021) 199–217, https://doi.org/10.1007/978-981-33-6753-1_9.

[192] B. Jain, S. Jain, R. Nema, Control strategies of grid interfaced wind energy conversion system: an overview, Renew. Sustain. Energy Rev. 47 (2015) 983–996, https://doi.org/10.1016/j.rser.2015.03.063.

[193] M. Prince, M. Arif, M. Haque, A. Gargoom, A. Oo, Design and implementation of finite control set mpc with an lcl filter for grid-tied pmsg based wind turbine, Int. J. Electr. Power Energy Syst. 152 (2023) 109197, https://doi.org/10.1016/j.ijepes.2023.109197.

[194] D.A. Gutiérrez-Torres, J.M. Ramírez, J.M. Lozano-García, Implementing a simplified power controller with a direct matrix converter for a pmsg-based wecs, IET Power Electron. 16 (16) (2023) 2782–2791, https://doi.org/10.1049/pel2.12601.

[195] I. Toumi, B. Meghni, O. Hachana, A.T. Azar, A. Boulmaiz, A.J. Humaidi, I.K. Ibraheem, N.A. Kamal, Q. Zhu, G. Fusco, et al., Robust variable-step perturb-and-observe sliding mode controller for grid-connected wind-energy-conversion systems, Entropy 24 (5) (2022) 731, https://doi.org/10.3390/e24050731.

[196] M. Benadja, M. Rezkallah, S. Benhalima, A. Hamadi, A. Chandra, Hardware testing of sliding mode controller for improved performance of vsc-hvdc based offshore wind farm under dc fault, IEEE Trans. Ind. Appl. 55 (2) (2018) 2053–2063, https://doi.org/10.1109/TIA.2018.2878539.

[197] K. Suleimenov, B. Sarsembayev, B. Duc Hong Phuc, T.D. Do, Disturbance observer-based integral sliding mode control for wind energy conversion systems, Wind Energy 23 (4) (2020) 1026–1047, https://doi.org/10.1002/we.2027.

[198] Y. Krim, D. Abbes, S. Krim, M.F. Mimouni, Classical vector, first-order sliding-mode and high-order sliding-mode control for a grid-connected variable-speed wind energy conversion system: a comparative study, Wind Eng. 42 (1) (2018) 16–37, https://doi.org/10.1177/0309524X17723202.

[199] B. Brahmi, M.H. Laraki, A. Brahmi, M. Saad, M.H. Rahman, Improvement of sliding mode controller by using a new adaptive reaching law: theory and experiment, ISA Trans. 97 (2020) 261–268, https://doi.org/10.1016/j.isatra.2019.08.010.

[200] S.M. Mozayan, M. Saad, H. Vahedi, H. Fortin-Blanchette, M. Soltani, Sliding mode control of pmsg wind turbine based on enhanced exponential reaching law, IEEE Trans. Ind. Electron. 63 (10) (2016) 6148–6159, https://doi.org/10.1109/TIE.2016.2570718.

[201] Y. Mousavi, G. Bevan, I.B. Küçükdemiral, A. Fekih, Maximum power extraction from wind turbines using a fault-tolerant fractional-order nonsingular terminal sliding mode controller, Energies 14 (18) (2021) 5887, https://doi.org/10.3390/en14185887.

[202] J. Talebi, S. Ganjefar, Fractional order sliding mode controller design for large scale variable speed wind turbine for power optimization, Environ. Prog. Sustain. Energy 37 (6) (2018) 2124–2131, https://doi.org/10.1002/ep.12878.

[203] G. Narayanan, M.S. Ali, Y.H. Joo, R. Perumal, B. Ahmad, H. Alsulami, Robust adaptive fractional sliding-mode controller design for Mittag-Leffler synchronization of fractional-order pmsg-based wind turbine system, IEEE Trans. Syst. Man Cybern. Syst. (2023), https://doi.org/10.1109/TSMC.2023.3296682.

[204] L. Xiong, P. Li, M. Ma, Z. Wang, J. Wang, Output power quality enhancement of pmsg with fractional order sliding mode control, Int. J. Electr. Power Energy Syst. 115 (2020) 105402, https://doi.org/10.1016/j.ijepes.2019.105402.

[205] V. Utkin, Discussion aspects of high-order sliding mode control, IEEE Trans. Autom. Control 61 (3) (2015) 829–833, https://doi.org/10.1109/TAC.2015.2450571.

[206] K. Mathiyalagan, G. Sangeetha, Second-order sliding mode control for nonlinear fractional-order systems, Appl. Math. Comput. 383 (2020) 125264, https://doi.org/10.1016/j.amc.2020.125264.

[207] X. Liu, Y. Han, Finite time control for mimo nonlinear system based on higher-order sliding mode, ISA Trans. 53 (6) (2014) 1838–1846, https://doi.org/10.1016/j.isatra.2014.09.002.

[208] H. Hou, X. Yu, L. Xu, R. Chuei, Z. Cao, Discrete-time terminal sliding-mode tracking control with alleviated chattering, IEEE/ASME Trans. Mechatron. 24 (4) (2019) 1808–1817, https://doi.org/10.1109/TMECH.2019.2928642.

[209] Y. Guo, B. Xu, R. Zhang, Terminal sliding mode control of mems gyroscopes with finite-time learning, IEEE Trans. Neural Netw. Learn. Syst. 32 (10) (2020) 4490–4498, https://doi.org/10.1109/TNNLS.2020.3018107.

[210] M. Nasiri, S. Mobayen, Q.M. Zhu, Super-twisting sliding mode control for gearless pmsg-based wind turbine, Complexity 2019 (2019), https://doi.org/10.1155/2019/6141607.

[211] A. Merabet, K.T. Ahmed, H. Ibrahim, R. Beguenane, Implementation of sliding mode control system for generator and grid sides control of wind energy conversion system, IEEE Trans. Sustain. Energy 7 (3) (2016) 1327–1335, https://doi.org/10.1109/TSTE.2016.2537646.

[212] F. Valenciaga, R.D. Fernandez, Multiple-input–multiple-output high-order sliding mode control for a permanent magnet synchronous generator wind-based system with grid support capabilities, IET Renew. Power Gener. 9 (8) (2015) 925–934, https://doi.org/10.1049/iet-rpg.2014.0417.

[213] X. Zheng, Y. Feng, F. Han, X. Yu, Integral-type terminal sliding-mode control for grid-side converter in wind energy conversion systems, IEEE Trans. Ind. Electron. 66 (5) (2018) 3702–3711, https://doi.org/10.1109/TIE.2018.2851959.

[214] S. Pradhan, B. Singh, B.K. Panigrahi, S. Murshid, A composite sliding mode controller for wind power extraction in remotely located solar pv–wind hybrid system, IEEE Trans. Ind. Electron. 66 (7) (2018) 5321–5331, https://doi.org/10.1109/TIE.2018.2868009.

[215] N.K. Jena, H. Pradhan, A. Choudhury, K. Mohanty, S. Sanyal, A novel smc based vector control strategy used for decoupled control of pmsg based variable speed wind turbine system, in: 2017 International Conference on Circuit, Power and Computing Technologies (ICCPCT), IEEE, 2017, pp. 1–6.

[216] D. Thakur, J. Jiang, Control of a pmsg wind-turbine under asymmetrical voltage sags using sliding mode approach, IEEE Power Energy Technol. Syst. J. 5 (2) (2018) 47–55, https://doi.org/10.1109/JPETS.2018.2825142.

[217] Y. Tang, J. Li, S. Li, Q. Cao, Y. Wu, Non-linear extended state observer-based sliding mode control for a direct-driven wind energy conversion system with permanent magnet synchronous generator, J. Eng. 2019 (15) (2019) 613–617, https://doi.org/10.1049/joe.2018.9392.

[218] M.M. Aghdam, L. Li, J. Zhu, Comprehensive study of finite control set model predictive control algorithms for power converter control in microgrids, IET Smart Grid 3 (1) (2020) 1–10, https://doi.org/10.1049/iet-stg.2018.0237.

[219] D. Razmi, O. Babayomi, A. Davari, T. Rahimi, Y. Miao, Z. Zhang, Review of model predictive control of distributed energy resources in microgrids, Symmetry 14 (8) (2022) 1735, https://doi.org/10.3390/sym14081735.

[220] I.M.-B. Hassine, M. Naouar, N. Mrabet-Bellaaj, Model based predictive control strategies for wind turbine system based on pmsg, in: IREC2015 the Sixth International Renewable Energy Congress, IEEE, 2015, pp. 1–6.

[221] D. Song, J. Yang, M. Dong, Y.H. Joo, Model predictive control with finite control set for variable-speed wind turbines, Energy 126 (2017) 564–572, https://doi.org/10.1016/j.energy.2017.02.149.

[222] A.A. Ghany, E. Shehata, A.-H.M. Elsayed, Y.S. Mohamed, H. Haes Alhelou, P. Siano, A.A.Z. Diab, Novel switching frequency fcs-mpc of pmsg for grid-connected wind energy conversion system with coordinated low voltage ride through, Electronics 10 (4) (2021) 492, https://doi.org/10.3390/electronics10040492.

[223] M. Abdelrahem, C. Hackl, R. Kennel, Robust predictive control scheme for permanent-magnet synchronous generators based modern wind turbines, Electronics 10 (13) (2021) 1596, https://doi.org/10.3390/electronics10131596.

[224] P. Kou, D. Liang, L. Yu, L. Gao, Nonlinear model predictive control of wind farm for system frequency support, IEEE Trans. Power Syst. 34 (5) (2019) 3547–3561, https://doi.org/10.1109/TPWRS.2019.2901741.

[225] I. Jlassi, A.J.M. Cardoso, Enhanced and computationally efficient model predictive flux and power control of pmsg drives for wind turbine applications, IEEE Trans. Ind. Electron. 68 (8) (2020) 6574–6583, https://doi.org/10.1109/TIE.2020.3005095.

[226] V. Yaramasu, B. Wu, Model Predictive Control of Wind Energy Conversion Systems, John Wiley & Sons, 2016.

[227] J. Wei, Y. Cao, Q. Wu, C. Li, S. Huang, B. Zhou, D. Xu, Coordinated droop control and adaptive model predictive control for enhancing hvrt and post-event recovery of large-scale wind farm, IEEE Trans. Sustain. Energy 12 (3) (2021) 1549–1560, https://doi.org/10.1109/TSTE.2021.3053955.

[228] B. Babaghorbani, M.T. Beheshti, H.A. Talebi, A Lyapunov-based model predictive control strategy in a permanent magnet synchronous generator wind turbine, Int. J. Electr. Power Energy Syst. 130 (2021) 106972, https://doi.org/10.1016/j.ijepes.2021.106972.

[229] Y. Guo, H. Gao, Q. Wu, J. Østergaard, D. Yu, M. Shahidehpour, Distributed coordinated active and reactive power control of wind farms based on model predictive control, Int. J. Electr. Power Energy Syst. 104 (2019) 78–88, https://doi.org/10.1016/j.ijepes.2018.06.043.

[230] S. Qin, Y. Chang, Z. Xie, S. Li, Improved virtual inertia of pmsg-based wind turbines based on multi-objective model-predictive control, Energies 14 (12) (2021) 3612, https://doi.org/10.3390/en14123612.

[231] Z. Guo, W. Wu, Data-driven model predictive control method for wind farms to provide frequency support, IEEE Trans. Energy Convers. 37 (2) (2021) 1304–1313, https://doi.org/10.1109/TEC.2021.3125369.

[232] I. Jlassi, A.J.M. Cardoso, Fault-tolerant back-to-back converter for direct-drive pmsg wind turbines using direct torque and power control techniques, IEEE Trans. Power Electron. 34 (11) (2019) 11215–11227, https://doi.org/10.1109/TPEL.2019.2897541.

[233] R. Errouissi, A. Al-Durra, M. Debouza, A novel design of pi current controller for pmsg-based wind turbine considering transient performance specifications and control saturation, IEEE Trans. Ind. Electron. 65 (11) (2018) 8624–8634, https://doi.org/10.1109/TIE.2018.2814007.

[234] S.A.R. Alsaadi, P.C. Matthews, C.J. Crabtree, Control strategy assessment for wind turbine converter reliability, https://doi.org/10.1049/icp.2022.1052, 2022.

[235] Y. Errami, A. Obbadi, S. Sahnoun, M. Ouassaid, M. Maaroufi, Direct torque control method applied to the wecs based on the pmsg and controlled with backstepping approach, in: AIP Conference Proceedings, vol. 1968, AIP Publishing LLC, 2018, p. 030020.

[236] S. Pradhan, S. Murshid, B. Singh, B.K. Panigrahi, Performance investigation of multifunctional on-grid hybrid wind–pv system with oasc and maf-based control, IEEE Trans. Power Electron. 34 (11) (2019) 10808–10822, https://doi.org/10.1109/TPEL.2019.2900759.

[237] R. Tiwari, K. Kumar, N.R. Babu, K. Prabhu, Coordinated mppt and dpc strategies for pmsg based grid connected wind energy conversion system, Energy Proc. 145 (2018) 339–344, https://doi.org/10.1016/j.egypro.2018.04.061.

[238] F. Louar, A. Ouari, A. Omeiri, F. Senani, A. Rahab, Direct power control (dpc) of pmsg based wind energy conversion system, in: 2015 4th International Conference on Electrical Engineering (ICEE), IEEE, 2015, pp. 1–6.

[239] Q. Xie, Z. Zheng, C. Huang, T. Dai, Coordinated fault ride through method for pmsg-based wind turbine using sfcl and modified control strategy, IEEE Trans. Appl. Supercond. 31 (8) (2021) 1–5, https://doi.org/10.1109/TASC.2021.3103730.

[240] J. Liu, F. Zhou, C. Zhao, Z. Wang, Mechanism analysis and suppression strategy research on permanent magnet synchronous generator wind turbine torsional vibration, ISA Trans. 92 (2019) 118–133, https://doi.org/10.1016/j.isatra.2019.02.006.

[241] M. Zoghlami, A. Kadri, F. Bacha, Analysis and application of the sliding mode control approach in the variable-wind speed conversion system for the utility of grid connection, Energies 11 (4) (2018) 720, https://doi.org/10.3390/en11040720.

[242] R. Moutchou, A. Abbou, Control of grid side converter in wind power based pmsg with pll method, Int. J. Power Electron. Drive Syst. 12 (4) (2021) 2191–2200, https://doi.org/10.11591/ijpeds.v12.i4.pp2191-2200.

[243] J. Liu, C. Zhao, Z. Xie, Power and current limiting control of wind turbines based on pmsg under unbalanced grid voltage, IEEE Access 9 (2021) 9873–9883, https://doi.org/10.1109/ACCESS.2021.3049839.

[244] A. Tounsi, H. Abid, Generator and grid side converter control for wind energy conversion system, Int. J. Power Electron. Drive Syst. 12 (3) (2021) 1832–1844, https://doi.org/10.11591/ijpeds.v12.i3.pp1832-1844.

[245] A.S. Bubshait, A. Mortezaei, M.G. Simoes, T.D.C. Busarello, Power quality enhancement for a grid connected wind turbine energy system, IEEE Trans. Ind. Appl. 53 (3) (2017) 2495–2505, https://doi.org/10.1109/TIA.2017.2657482.

[246] M.A. Soliman, H.M. Hasanien, A. Al-Durra, M. Debouza, High performance frequency converter controlled variable-speed wind generator using linear-quadratic regulator controller, IEEE Trans. Ind. Appl. 56 (5) (2020) 5489–5498, https://doi.org/10.1109/TIA.2020.2996956.

[247] M. Jahanpour-Dehkordi, S. Vaez-Zadeh, J. Mohammadi, Development of a combined control system to improve the performance of a pmsg-based wind energy conversion system under normal and grid fault conditions, IEEE Trans. Energy Convers. 34 (3) (2019) 1287–1295, https://doi.org/10.1109/TEC.2019.2912080.

[248] M.H. Qais, H.M. Hasanien, S. Alghuwainem, A grey wolf optimizer for optimum parameters of multiple pi controllers of a grid-connected pmsg driven by variable speed wind turbine, IEEE Access 6 (2018) 44120–44128, https://doi.org/10.1109/ACCESS.2018.2864303.

[249] Y. Mousavi, G. Bevan, I.B. Kucukdemiral, A. Fekih, Sliding mode control of wind energy conversion systems: trends and applications, Renew. Sustain. Energy Rev. 167 (2022) 112734, https://doi.org/10.1016/j.rser.2022.112734.

[250] S.M. Tripathi, A.N. Tiwari, D. Singh, Controller design for a variable-speed direct-drive permanent magnet synchronous generator-based grid-interfaced wind energy conversion system using d-partition technique, IEEE Access 5 (2017) 27297–27310, https://doi.org/10.1109/ACCESS.2017.2775250.

[251] W. Cao, N. Xing, Y. Wen, X. Chen, D. Wang, New adaptive control strategy for a wind turbine permanent magnet synchronous generator (pmsg), Inventions 6 (1) (2021) 3, https://doi.org/10.3390/inventions6010003.

[252] M.A. Soliman, H.M. Hasanien, A. Al-Durra, I. Alsaidan, A novel adaptive control method for performance enhancement of grid-connected variable-speed wind generators, IEEE Access 8 (2020) 82617–82629, https://doi.org/10.1109/ACCESS.2020.2991689.

[253] M.I. Mosaad, H.S.M. Ramadan, M. Aljohani, M.F. El-Naggar, S.S. Ghoneim, Near-optimal pi controllers of statcom for efficient hybrid renewable power system, IEEE Access 9 (2021) 34119–34130, https://doi.org/10.1109/ACCESS.2021.3058081.

[254] T. Magesh, G. Devi, T. Lakshmanan, Improving the performance of grid connected wind generator with a pi control scheme based on the metaheuristic golden eagle optimization algorithm, Electr. Power Syst. Res. 214 (2023) 108944, https://doi.org/10.1016/j.epsr.2022.108944.

[255] M.H. Qais, H.M. Hasanien, S. Alghuwainem, Augmented grey wolf optimizer for grid-connected pmsg-based wind energy conversion systems, Appl. Soft Comput. 69 (2018) 504–515, https://doi.org/10.1016/j.asoc.2018.05.006.

[256] N.A. Mohamed, H.M. Hasanien, E.A. Al-Ammar, M. Tostado-Véliz, R.A. Turky, F. Jurado, A.O. Badr, Gorilla tropical optimization algorithm solution for performance enhancement of offshore wind farm, IET Gener. Transm. Distrib. 17 (10) (2023) 2388–2400, https://doi.org/10.1109/IREC.2018.8362516.

[257] B. Yang, T. Yu, H. Shu, X. Zhang, K. Qu, L. Jiang, Democratic joint operations algorithm for optimal power extraction of pmsg based wind energy conversion system, Energy Convers. Manag. 159 (2018) 312–326, https://doi.org/10.1016/j.enconman.2017.12.090.

[258] M.M. Mahmoud, M.K. Ratib, M.M. Aly, A.-M.M. Abdel-Rahim, Application of whale optimization technique for evaluating the performance of wind-driven pmsg under harsh operating events, Process Integration Optim. Sustain. 6 (2) (2022) 447–470, https://doi.org/10.1007/s41660-022-00224-8.

[259] Y.-S. Kim, I.-Y. Chung, S.-I. Moon, Tuning of the pi controller parameters of a pmsg wind turbine to improve control performance under various wind speeds, Energies 8 (2) (2015) 1406–1425, https://doi.org/10.3390/en8021406.

[260] M.H. Qais, H.M. Hasanien, S. Alghuwainem, Optimal transient search algorithm-based pi controllers for enhancing low voltage ride-through ability of grid-linked pmsg-based wind turbine, Electronics 9 (11) (2020) 1807, https://doi.org/10.3390/electronics9111807.

[261] M.A. Soliman, H.M. Hasanien, S. Alghuwainem, A. Al-Durra, Symbiotic organisms search algorithm-based optimal control strategy for efficient operation of variable-speed wind generators, IET Renew. Power Gener. 13 (14) (2019) 2684–2692, https://doi.org/10.1049/iet-rpg.2019.0834.

[262] H. Shutari, N. Saad, N.B.M. Nor, M.F.N. Tajuddin, A. Alqushaibi, M.A. Magzoub, Towards enhancing the performance of grid-tied vswt via adopting sine cosine algorithm-based optimal control scheme, IEEE Access 9 (2021) 139074–139088, https://doi.org/10.1109/ACCESS.2021.3119019.

[263] H. Shutari, T. Ibrahim, N.B.M. Nor, H. Abdulrab, N. Saad, Q. Al-Tashi, Coordination of enhanced control schemes for optimal operation and ancillary services of grid-tied vswt system, IEEE Access (2023), https://doi.org/10.1109/ACCESS.2023.3272000.

[264] Y. Belkhier, N. Ullah, A.A. Al Alahmadi, Efficiency maximization of grid-connected tidal stream turbine system: a supervisory energy-based speed control approach with processor in the loop experiment, Sustainability 13 (18) (2021) 10216, https://doi.org/10.3390/su131810216.

[265] Y. Belkhier, A. Achour, R.N. Shaw, Fuzzy passivity-based voltage controller strategy of grid-connected pmsg-based wind renewable energy system, in: 2020 IEEE 5th International Conference on Computing Communication and Automation (ICCCA), IEEE, 2020, pp. 210–214.

[266] A. Jaiswal, Y. Belkhier, S. Chandra, A. Priyadarshi, M. Bajaj, M. Pushkarna, E. Elgamli, M. Shouran, S. Kamel, Design and implementation of energy reshaping based fuzzy logic control for optimal power extraction of pmsg wind energy converter, Frontiers Energy Res. 10 (2022) 966975, https://doi.org/10.3389/fenrg.2022.966975.

[267] Y. Belkhier, A. Achour, R.N. Shaw, A. Ghosh, Performance improvement for pmsg tidal power conversion system with fuzzy gain supervisor passivity-based current control, in: Innovations in Electrical and Electronic Engineering: Proceedings of ICEEE 2021, Springer, 2021, pp. 81–93.

[268] M.A. Soliman, H.M. Hasanien, H.Z. Azazi, E.E. El-kholy, S.A. Mahmoud, Hybrid anfis-ga-based control scheme for performance enhancement of a grid-connected wind generator, IET Renew. Power Gener. 12 (7) (2018) 832–843, https://doi.org/10.1049/iet-rpg.2017.0576.

[269] H.H. Mousa, A.-R. Youssef, E.E. Mohamed, Model predictive speed control of five-phase permanent magnet synchronous generator-based wind generation system via wind-speed estimation, Int. Trans. Electr. Energy Syst. 29 (5) (2019) e2826, https://doi.org/10.1002/2050-7038.2826.

[270] M.H. Qais, H.M. Hasanien, S. Alghuwainem, A novel lmsre-based adaptive pi control scheme for grid-integrated pmsg-based variable-speed wind turbine, Int. J. Electr. Power Energy Syst. 125 (2021) 106505, https://doi.org/10.1016/j.ijepes.2020.106505.

[271] Y. Zhu, Z. Ma, Z. Wang, An improved fuzzy logic based dc-link voltage control strategy for smoothing output power of the pmsg-wecs, Energy Rep. 8 (2022) 8413–8425, https://doi.org/10.1016/j.egyr.2022.06.049.

[272] R. Venkateswaran, A.A. Yesudhas, S.R. Lee, Y.H. Joo, Integral sliding mode control for extracting stable output power and regulating dc-link voltage in pmvg-based wind turbine system, Int. J. Electr. Power Energy Syst. 144 (2023) 108482, https://doi.org/10.1016/j.ijepes.2022.108482.